

Lanthanide-Catalyst-Mediated Tandem Double Intramolecular Hydroalkoxylation/Cyclization of Dialkynyl Dialcohols: Scope and Mechanism

SungYong Seo and Tobin J. Marks^{*[a]}

Abstract: Lanthanide-organic complexes of the general type $[\text{Ln}(\text{N}(\text{SiMe}_3)_2)_3]$ ($\text{Ln} = \text{La}, \text{Sm}, \text{Y}, \text{Lu}$) serve as effective precatalysts for the rapid, *exo*-selective, and highly regioselective tandem double intramolecular hydroalkoxylation/cyclization of primary and secondary dialkynyl dialcohols to yield the corresponding bi-exocyclic enol ethers. Conversions are highly selective with products distinctly different from those generally produced by conventional transition metal or other catalysts, and the turnover frequencies with some substrates are too large to determine accurately. The rates of terminal

alkynyl alcohol hydroalkoxylation/cyclization are significantly more rapid than those of internal alkynyl alcohols, arguing that steric demands dominate the cyclization transition state. The hydroalkoxylation/cyclizations of internal dialkynyl dialcohols afford excellent *E* selectivity. The rate law for dialkynyl dialcohol hydroalkoxylation/cyclization is first-order in [catalyst] and zero-

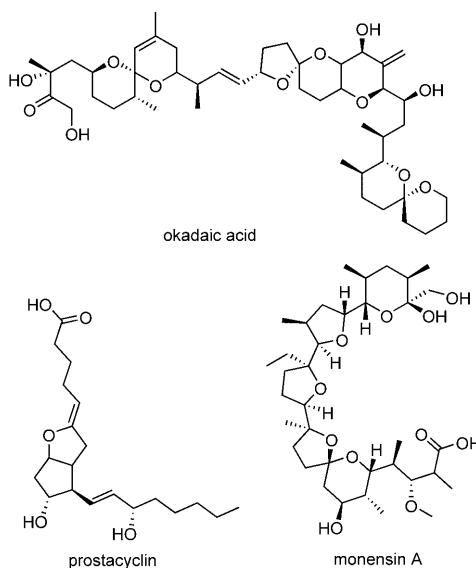
Keywords: heterogeneous catalysis • hydroalkoxylation • lanthanides • oxygen heterocycles • parallel reactions

order in [alkynyl alcohol], as is observed for the organolanthanide-catalyzed hydroamination/cyclization of aminoalkenes, aminoalkynes, and aminoallenes, and the intramolecular single-step hydroalkoxylation/cyclization of alkynyl alcohols. An ROH/ROD kinetic isotope effect of 0.82(0.02) is observed for the tandem double hydroalkoxylation/cyclization. These mechanistic data implicate turnover-limiting insertion of C–C unsaturation into the Ln–O bond, involving a highly organized transition state, with subsequent, rapid Ln–C protonolysis.

Introduction

Oxygen-containing heterocycles are important structural motifs in many naturally occurring and pharmacologically active organic molecules (e.g., okadaic acid, prostacyclin, and monensin A).^[1] For this reason, the constraints of traditional heterocycle synthetic methodologies have stimulated great interest in the development of new, more efficient and selective homogeneous catalytic approaches to important heterocyclic frameworks.^[2] In principle, many important and useful oxygen-containing organic structures should be accessible via catalytic hydroalkoxylation of alkenes or alkynes using transition metal or other catalysts,^[3] and effective in-

tramolecular variants of this reaction would provide straightforward and atom-efficient approaches to numerous



[a] Dr. S. Seo, Prof. Dr. T. J. Marks

Department of Chemistry, Northwestern University
Evanston, Illinois 60208 (USA)
E-mail: t-marks@northwestern.edu

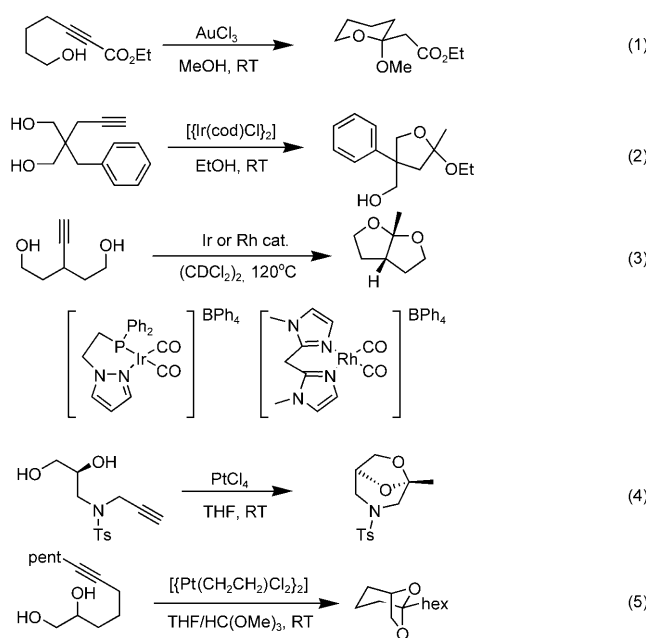
Supporting information for this article is available on the WWW under <http://dx.doi.org/10.1002/chem.200903027>: Complete experimental procedure and spectral data for all synthetic compounds; ¹H and ¹³C NMR spectra of representative compounds.

oxygen-containing heterocycles. However, while catalytic hydroalkoxylation offers many attractions versus traditional heterocycle synthetic pathways, efficient catalytic transformations present many challenges due to several factors, such as the relatively large bond enthalpies of typical O–H bonds and the modest reactivity of electron-rich olefins with nucleophiles.

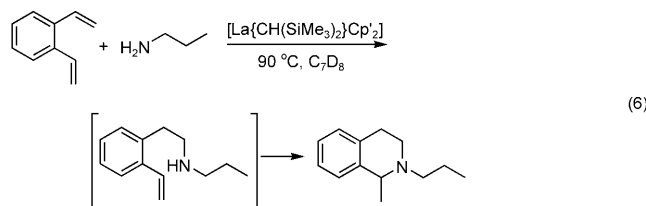
In pursuit of the “ideal synthesis”, the concept of efficiency is not limited simply to high yields but is, in fact, multi-faceted.^[4] Over the past several years, significant research activity has focused on developing new bond-forming methodologies which enhance synthetic efficiency and atom economy.^[5] Among these, tandem reactions which promote formation of several new bonds in a single sequence from readily available starting materials are of particular interest.^[6] Processes that form multiple carbon–carbon or carbon–heteroatom bonds in a sequence of events without inefficient isolation of intermediates represent a powerful means to approach this ideality. In this context, concurrent tandem reactions provide a means to improve synthetic efficiency and chemoselectivity. In terms of hydrofunctionalization, there has therefore been great interest in developing more efficient and selective single-site hydroalkoxylation catalysts to mediate such challenging transformation sequences.^[7–10]

There have been growing efforts to develop catalysts for tandem hydroalkoxylation. Most of these transformations produce cyclic or bicyclic acetals using transition-metal catalysts via intermolecular or intramolecular pathways. Tandem intermolecular hydroalkoxylation processes include the formation of cyclic acetals from alkynyl alcohols and another alcohol such as MeOH or EtOH using AuCl₃,^[11] [AuCl(Ph₃P)],^[12] or [{Ir(cod)Cl}₂] catalysts [e.g., Eqs. (1) and (2)].^[13] Intramolecular processes include the formation of bicyclic acetals from alkynyl dialcohols using [AuCl(Ph₃P)],^[14] Rh,^[15] or Ir catalysts [Eq. (3)].^[16] For example, Ley’s and De Brabander’s groups used PtCl₄ [Eq. (4)]^[17] and [{Pt(CH₂CH₂)Cl₂}]^[18] catalysts to produce fused bicyclic acetals from alkynyl dialcohols. However, to the best of our knowledge, tandem intramolecular C–O fusion processes using two alkynyl groups and two alcohol functionalities have never been reported.

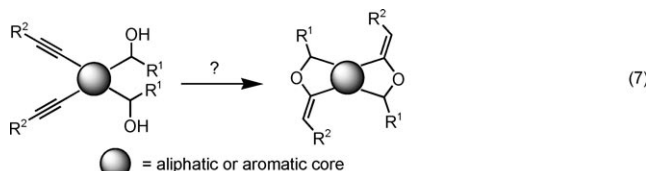
Organolanthanide complexes are known to be highly active hydrofunctionalization catalysts.^[19–21] Among such catalysts, easily prepared homoleptic [Ln{N(SiMe₃)₂}₃] amido complexes (Ln = lanthanide, Y)^[22] are versatile agents for a variety of organic transformations, which can be either intermolecular or intramolecular in character. Successful intermolecular transformations include ynene synthesis,^[23] cross-aldol reactions,^[24] coupling of isocyanides with terminal alkynes,^[25] dimerization of terminal alkynes,^[26] guanylation of amines,^[27] hydrosilylation,^[28] hydroboration,^[29] Tishchenko aldehyde dimerization,^[30] and amidations.^[31] Intramolecular transformations include hydroelementation processes, such as hydroamination,^[32,30b] hydrophosphination,^[20b] and hydroalkoxylation.^[33] In regard to organolanthanide-mediated tandem hydrofunctionalization processes, several very effi-



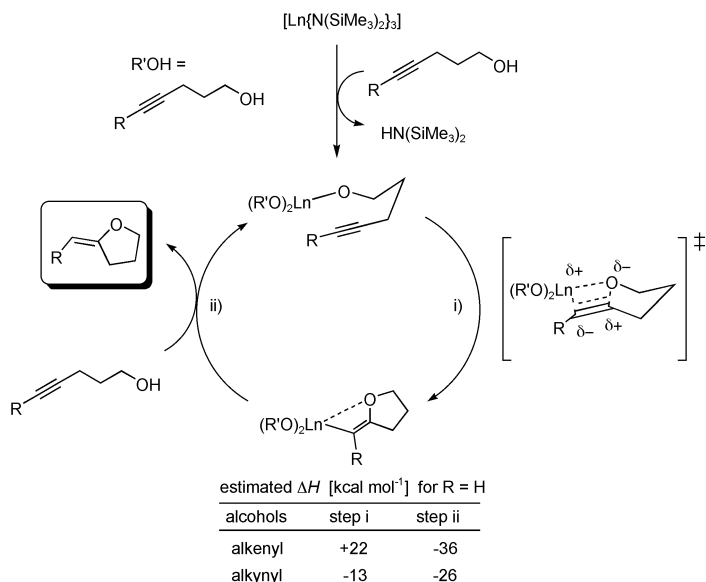
cient and selective hydroamination/C–C bond formation sequences have been reported [e.g., Eq. (6)].^[32c]



We recently reported a detailed study of the scope, kinetics, and mechanism of the catalytic intramolecular single hydroalkoxylation/cyclization of a broad series terminal and internal monoalkynyl alcohols.^[33] In that work we showed that internal alkynyl alcohols are transformed exclusively to *exo*-enol ethers as shown in Scheme 1 with thermodynamic considerations.^[34] Herein we report a detailed scope/kinetic/mechanistic study aimed at determining whether and with what scope, catalytic dialkynyl dialcohol tandem double hydroalkoxylation processes can be effected [Eq. (7)]. Al-



though the catalytic synthesis of such target structures has never been reported, these structures should be very useful scaffolds, with a variety of applications in natural and pharmaceutical product synthesis. Note that structurally similar



Scheme 1. Catalytic cycle for lanthanide-mediated single hydroalkoxylation/cyclization of internal alkynyl alcohols.

structures such as *O,O*-spiroacetals,^[35] omaezakianol,^[36] and gymnocin A^[37] are prevalent in natural products. In this account, substrate synthetic routes, reaction scope, stereoselectivity, metal ion effects, and reaction kinetics and mechanism are examined in detail and compared/contrasted with previously characterized intramolecular hydroalkoxylation/-, intramolecular hydroamination/-, and hydrophosphination/-cyclization processes.

Experimental Section

Materials and methods: All manipulations of air-sensitive materials were carried out with rigorous exclusion of oxygen and moisture in flame- or oven-dried Schlenk-type glassware on a dual-manifold Schlenk line, interfaced to a high-vacuum line (10^{-6} Torr), or in a nitrogen-filled vacuum atmospheres glove box with a high capacity recirculator (<1 ppm of O₂). Argon (Airgas, prepurified) was purified by passage through a MnO oxygen-removal column and a Davison 4 Å molecular sieves column. Pentane was dried using activated alumina columns according to the method described by Grubbs.^[38] Et₂O and THF were distilled from sodium/benzophenone. Benzene was dried by vacuum-transfer from Na/K alloy immediately prior to use if employed for catalyst synthesis or catalytic reactions. D₂O (Cambridge Isotope Laboratories; all 99+ atom % D) was used directly as received. [D₆]-Benzene and [D₁₀]-*o*-xylene (Cambridge Isotope Laboratories; all 99+ atom % D) used for NMR reactions and kinetic measurements were stored in vacuo over Na/K alloy in re-sealable bulbs and were vacuum-transferred immediately prior to use. Substrates **1**,^[39] **7**,^[40] **9**,^[41] **27**,^[42] and **29**,^[41,42] were prepared as reported in the literature. All liquid substrates were dried twice as solutions in [D₆]-benzene over freshly activated Davison 4 Å molecular sieves and were degassed by freeze-pump-thaw methods. They were then stored in vacuum-tight storage flasks. Solid substrates were sublimed under high-vacuum and stored in the glove box before use. The lanthanide complexes [Ln{N(SiMe₃)₂}₃] (Ln=La, Nd, Sm, Y, and Lu), were prepared according to published procedures.^[22] Details of substrate syntheses and characterization are provided in the Supporting Information.

Physical and analytical measurements: NMR spectra were recorded on a Varian Gemini 300 (300 MHz, ¹H; 75 MHz, ¹³C), Mercury-400 (FT,

400 MHz, ¹H; 100 MHz, ¹³C), or Inova-500 (500 MHz, ¹H; 125 MHz, ¹³C, 76.7 MHz, ²H) instrument. Chemical shifts (δ) for ¹H, ²H, and ¹³C are referenced to internal solvent resonances and reported relative to SiMe₄. NMR experiments on air-sensitive samples were conducted in Teflon valve-sealed J. Young tubes. Mass spectra data were obtained on a Varian 1200 Quadrupole Mass Spectrometer and Micromass Quadro II Spectrometer. Elemental analyses were performed by Midwest Micro-labs, Indianapolis, IN.

1-(2,5-Diethynyl-4-(hydroxymethyl)phenyl)ethanol (11): ¹H NMR (400 MHz, CDCl₃): δ =7.67 (s, 1H), 7.54 (s, 1H), 5.28 (q, J =6.3 Hz, 1H), 4.77 (s, 2H), 3.39 (s, 2H), 1.94 (br, 2H), 1.47 ppm (d, J =6.3 Hz, 3H); ¹³C NMR (100 MHz, CDCl₃): δ =147.38, 141.85, 131.56, 129.33, 119.97, 83.83, 83.49, 80.78, 67.79, 63.09, 23.97 ppm; elemental analysis calcd (%) for C₁₃H₁₂O₂: C 77.98, H 6.04; found: C 77.88, H 6.08.

1,1'-(2,5-Diethynyl-1,4-phenylene)diethanol (13): ¹H NMR (400 MHz, CDCl₃): δ =7.64 (s, 2H), 5.26 (q, J =6.3 Hz, 2H), 3.39 (s, 2H), 2.03 (s, 2H), 1.47 ppm (d, J =6.3 Hz, 6H); ¹³C NMR (100 MHz, CDCl₃): δ =148.24, 129.68, 115.71, 83.89, 68.02, 24.16 ppm; elemental analysis calcd (%) for C₁₄H₁₄O₂: C 78.48, H 6.59; found: C 78.24, H 6.78.

(4,6-Diethynyl-1,3-phenylene)dimethanol (15): ¹H NMR (400 MHz, [D₆]DMSO): δ =7.71 (s, 1H), 7.41 (s, 1H), 5.37 (t, J =5.9 Hz, 2H), 4.59 (d, J =5.5 Hz, 4H), 4.38 (s, 2H), 2.26 (t, J =5.5 Hz, 2H), 2.04 ppm (t, J =2.8 Hz, 1H); ¹³C NMR (100 MHz, [D₆]DMSO): δ =145.69, 135.36, 124.56, 117.71, 85.94, 80.41, 61.37 ppm; elemental analysis calcd (%) for C₁₂H₁₀O₂: C 77.40, H 5.41; found: C 77.25, H 5.31.

1,1'-(4,6-Diethynyl-1,3-phenylene)diethanol (17): ¹H NMR (400 MHz, CDCl₃): δ =7.67 (s, 1H), 7.48 (s, 1H), 5.20 (m, 2H), 3.25 (s, 2H), 2.83 (br, 2H), 1.41 ppm (d, J =3.9 Hz, 6H); ¹³C NMR (100 MHz, CDCl₃): δ =152.26, 152.19, 139.74, 139.55, 123.63, 123.42, 120.52, 85.00, 84.90, 82.88, 70.62, 70.43, 26.56 ppm; elemental analysis calcd (%) for C₁₄H₁₄O₂: C 78.48, H 6.59; found: C 77.98, H 6.67.

(3,6-Diethynyl-1,2-phenylene)dimethanol (19): ¹H NMR (400 MHz, CDCl₃): δ =7.44 (s, 2H), 5.00 (d, J =6.3 Hz, 4H), 3.37 (s, 2H), 2.84 ppm (t, J =6.3 Hz, 2H); ¹³C NMR (100 MHz, CDCl₃): δ =142.15, 132.57, 123.38, 83.00, 81.08, 61.03 ppm; elemental analysis calcd (%) for C₁₂H₁₀O₂: C 77.40, H 5.41; found: C 77.40, H 5.50.

2-(But-2-ynyl)-2-(prop-2-ynyl)propane-1,3-diol (21): ¹H NMR (400 MHz, CDCl₃): δ =3.68 (d, J =5.5 Hz, 4H), 2.42 (t, J =5.5 Hz, 2H), 2.31 (d, J =2.3 Hz, 2H), 2.24 (m, 2H), 2.01 (t, J =2.7 Hz, 1H), 1.76 ppm (t, J =2.3 Hz, 3H); ¹³C NMR (100 MHz, CDCl₃): δ =80.79, 78.82, 74.84, 71.20, 66.95, 42.39, 22.37, 21.98, 3.74 ppm; elemental analysis calcd (%) for C₁₀H₁₄O₂: C 72.26, H 8.49; found: C 72.02, H 8.49.

2-(Prop-2-ynyl)-2-(3-(trimethylsilyl)prop-2-ynyl)propane-1,3-diol (22): ¹H NMR (400 MHz, CDCl₃): δ =3.72 (d, J =4.7 Hz, 4H), 2.34 (s, 4H), 2.25 (q, J =5.5 Hz, 2H), 2.02 (t, J =2.7 Hz, 1H), 0.13 ppm (s, 9H); ¹³C NMR (100 MHz, CDCl₃): δ =80.42, 71.40, 71.37, 66.91, 66.74, 42.37, 23.61, 22.10, 21.91, 0.23 ppm; elemental analysis calcd (%) for C₁₂H₂₀O₂Si: C 64.24, H 8.98; found: C 67.55, H 8.48.

2-(3-Phenylprop-2-ynyl)-2-(prop-2-ynyl)propane-1,3-diol (23): ¹H NMR (400 MHz, CDCl₃): δ =7.37 (m, 2H), 7.26 (m, 3H), 3.78 (d, J =6.3 Hz, 4H), 2.55 (s, 2H), 2.41 (d, J =3.1 Hz, 2H), 2.26 (t, J =5.5 Hz, 2H), 2.04 ppm (t, J =2.8 Hz, 1H); ¹³C NMR (100 MHz, CDCl₃): δ =131.81, 128.49, 128.18, 123.51, 85.78, 83.57, 80.62, 71.43, 67.06, 42.75, 23.02, 22.15 ppm; elemental analysis calcd (%) for C₁₅H₁₆O₂: C 78.92, H 7.06; found: C 79.10, H 7.16.

1-(4-(Hydroxymethyl)-2,5-bis(phenylethynyl)ethanol (33): ¹H NMR (400 MHz, [D₆]DMSO): δ =7.66 (s, 1H), 7.57 (s, 1H), 7.40 (m, 4H), 7.27 (m, 6H), 5.18 (m, 1H), 4.93 (m, 2H), 4.71 (d, J =5.5 Hz, 2H), 1.37 ppm (d, J =6.3 Hz, 3H); ¹³C NMR (100 MHz, [D₆]DMSO): δ =147.62, 142.15, 131.44, 131.34, 129.76, 128.63, 128.58, 128.55, 128.39, 122.94, 120.53, 119.88, 95.22, 87.49, 87.20, 66.72, 61.64, 24.97 ppm; elemental analysis calcd (%) for C₂₅H₂₀O₂: C 85.20, H 5.72; found: C 83.44, H 5.97.

1,1'-(2,5-Bis(phenylethynyl)-1,4-phenylene)diethanol (35): ¹H NMR (400 MHz, [D₆]DMSO): δ =7.66 (m, 2H), 7.55 (m, 4H), 7.42 (m, 6H), 5.35 (m, 2H), 5.14 (br, 2H), 1.37 ppm (m, 6H); ¹³C NMR (100 MHz, [D₆]DMSO): δ =150.75, 149.68, 135.42, 134.38, 133.91, 132.14, 131.97, 125.76, 125.26, 123.21, 122.59, 114.27, 98.24, 92.20, 90.22, 87.44, 69.11,

67.19, 33.50, 28.00 ppm; elemental analysis calcd (%) for $C_{26}H_{22}O_2$: C 85.22, H 6.05; found: C 84.92, H 6.32.

(4,6-Bis(phenylethynyl)-1,3-phenylene)dimethanol (37): 1H NMR (400 MHz, $CDCl_3$): δ = 7.68 (s, 1H), 7.62 (s, 1H), 7.46 (m, 4H), 7.30 (m, 6H), 4.87 (s, 4H), 3.74 ppm (s, 2H); ^{13}C NMR (100 MHz, $CDCl_3$): δ = 143.47, 135.20, 131.51, 128.54, 125.34, 122.82, 119.80, 94.33, 85.97, 63.14 ppm; elemental analysis calcd (%) for $C_{24}H_{18}O_2$: C 85.18, H 5.36; found: C 79.82, H 5.33.

1,1'-(4,6-Bis(phenylethynyl)-1,3-phenylene)diethanol (39): *meso/D,L*: 1H NMR (400 MHz, $CDCl_3$): δ = 7.66 (s, 1H), 7.50 (m, 2H), 7.45 (m, 3H), 7.35 (m, 2H), 7.29 (m, 4H), 5.37 (m, 2H), 3.26 (br, 2H), 1.54 ppm (m, 6H); ^{13}C NMR (100 MHz, $CDCl_3$): δ = 148.23, 148.09, 135.86, 135.55, 131.46, 128.61, 128.46, 128.34, 123.02, 121.19, 119.33, 118.91, 94.62, 94.42, 86.17, 86.08, 68.57, 68.49, 24.20, 24.01 ppm; elemental analysis calcd (%) for $C_{26}H_{22}O_2$: C 85.22, H 6.05; found: C 80.62, H 5.86.

(3,6-Bis(phenylethynyl)-1,2-phenylene)dimethanol (41): 1H NMR (400 MHz, $CDCl_3$): δ = 7.52 (m, 4H), 7.50 (s, 2H), 7.34 (m, 6H), 5.08 (d, J = 6.3 Hz, 4H), 2.94 ppm (t, J = 6.3 Hz, 2H); ^{13}C NMR (100 MHz, $CDCl_3$): δ = 144.12, 134.71, 134.29, 131.39, 131.10, 126.62, 125.36, 97.68, 89.73, 64.05 ppm; elemental analysis calcd (%) for $C_{24}H_{18}O_2$: C 85.18, H 5.36; found: C 82.50, H 5.30.

Typical NMR-scale catalytic reactions: In the glove box, the particular homoleptic lanthanide amide [$Ln[N(SiMe_3)_2]_3$] (5 μ mol) and the substrate (0.1 mmol) were weighed into separate vials, and $[D_6]$ -benzene (300 μ L) or $[D_{10}]$ -*o*-xylene was added by syringe to each vial. The solutions were then mixed to yield a homogeneous, clear solution which was then transferred to a J. Young NMR tube equipped with a Teflon valve. The tube was closed and removed from the glove box. The NMR tube was next sealed and frozen at $-78^\circ C$ until the time for NMR analysis, then brought to the desired temperature, and the ensuing hydroalkoxylation/cyclization reaction was monitored by 1H NMR spectroscopy.

Typical preparative-scale catalytic reactions: Scale-up catalytic reactions were carried out using the following procedure. In a glove box, the particular homoleptic lanthanide amide [$La[N(SiMe_3)_2]_3$] (31 mg, 50 μ mol) and the substrate (1 mmol) were weighed into separate vials, and 400 μ L of $[D_6]$ -benzene or $[D_{10}]$ -*o*-xylene was added by syringe to each vial. The reagents were then mixed to yield a homogeneous, clear solution and transferred to a solvent storage tube equipped with a Teflon valve and a magnetic stir bar. The tube was next closed and removed from the glove box. The mixture was then freeze-pump-thaw degassed and warmed to room temperature. The resulting solution was stirred with heating at the selected temperature for 12 h. After completion of the reaction, this reaction mixture was filtered through a small plug of silica gel to remove the catalyst. This crude product was then purified by flash column chromatography or Kugelrohr distillation.

3,8-Dimethylene-2,7-dioxaspiro[4.4]nonane (2): 1H NMR (400 MHz, C_6D_6): δ = 4.42 (s, 2H), 3.76 (s, 2H), 3.37 (s, 4H), 1.91 ppm (s, 4H); ^{13}C NMR (100 MHz, C_6D_6): δ = 161.53, 81.03, 76.43, 47.99, 38.25 ppm; HRMS-ESI: *m/z*: calcd for $C_9H_{13}O_2$: 153.0916; found: 153.0908 [$M+H^+$].

meso-1,9-Dimethyl-3,7-dimethylene-2,8-dioxaspiro[4.4]nonane (4): 1H NMR (400 MHz, $[D_{10}]$ -*o*-xylene): δ = 4.43 (s, 2H), 4.11 (m, 2H), 3.87 (s, 2H), 1.53 (s, 4H), 1.01 ppm (d, J = 6.3 Hz, 6H); ^{13}C NMR (100 MHz, $[D_{10}]$ -*o*-xylene): δ = 162.49, 87.55, 77.76, 50.35, 42.94, 25.24 ppm; HRMS-ESI: *m/z*: calcd for $C_{11}H_{16}O_2$: 203.1048; found: 203.1040 [$M+Na^+$].

d,l-1,9-Dimethyl-3,7-dimethylene-2,8-dioxaspiro[4.4]nonane (6): 1H NMR (400 MHz, $[D_{10}]$ -*o*-xylene): δ = 5.02 (s, 2H), 4.46 (s, 2H), 4.38 (q, J = 6.6 Hz, 2H), 2.65 (s, 4H), 1.68 ppm (d, J = 6.3 Hz, 6H); ^{13}C NMR (100 MHz, $[D_{10}]$ -*o*-xylene): δ = 168.81, 87.32, 77.39, 51.33, 42.64, 27.72 ppm; HRMS-ESI: *m/z*: calcd for $C_{11}H_{16}NaO_2$, 204.1048; found: 203.1038 [$M+Na^+$].

3,7-Dimethylene-1,5-dihydrofuro[3,4-*f*]isobenzofuran (10): 1H NMR (400 MHz, C_6D_6): δ = 6.52 (s, 2H), 4.70 (s, 4H), 4.68 (s, 2H), 4.44 ppm (s, 2H); ^{13}C NMR (100 MHz, C_6D_6): δ = 161.64, 140.76, 135.14, 113.43, 78.77, 72.96 ppm; HRMS-ESI: *m/z*: calcd for $C_{12}H_{11}O_2$: 187.0759; found: 187.0749 [$M+H^+$].

3-Methyl-1,5-dimethylene-3,7-dihydrofuro[3,4-*f*]isobenzofuran (12): 1H NMR (400 MHz, C_6D_6): δ = 6.73 (s, 1H), 6.54 (s, 1H), 5.19 (q, J =

6.3 Hz, 1H), 4.71 (s, 2H), 4.70 (s, 1H), 4.67 (s, 1H), 4.48 (s, 1H), 4.44 (s, 1H), 1.12 ppm (d, J = 6.3 Hz, 3H); ^{13}C NMR (100 MHz, C_6D_6): δ = 164.10, 163.03, 147.90, 143.38, 137.66, 115.94, 115.66, 82.72, 81.21, 81.11, 75.41, 23.75 ppm; HRMS-ESI: *m/z*: calcd for $C_{13}H_{13}O_2$: 201.0916; found: 201.0908 [$M+H^+$].

1,5-Dimethyl-3,7-dimethylene-1,5-dihydrofuro[3,4-*f*]isobenzofuran (14):

1H NMR (400 MHz, C_6D_6): δ = 6.75 (d, J = 4.7 Hz, 2H), 5.12 (q, J = 5.5 Hz, 2H), 4.68 (s, 2H), 4.48 (s, 2H), 1.13 ppm (t, J = 5.5 Hz, 6H); ^{13}C NMR (100 MHz, C_6D_6): δ = 160.42, 145.42, 135.02, 113.11, 113.09, 80.09, 78.47, 21.10 ppm; HRMS-ESI: *m/z*: calcd for $C_{14}H_{15}O_2$: 215.1072; found: 215.1062 [$M+H^+$].

3,5-Dimethylene-1,7-dihydrofuro[3,4-*f*]isobenzofuran (16): 1H NMR (400 MHz, C_6D_6): δ = 7.33 (s, 1H), 5.97 (s, 1H), 4.69 (s, 6H), 4.48 ppm (s, 2H); ^{13}C NMR (100 MHz, C_6D_6): δ = 163.86, 144.13, 136.94, 116.51, 115.02, 81.15, 75.29 ppm; HRMS-ESI: *m/z*: calcd for $C_{12}H_{11}O_2$: 187.0759; found: 187.0747 [$M+H^+$].

3,5-Dimethylene-1,7-dimethylene-3,5-dihydrofuro[3,4-*f*]isobenzofuran (18):

1H NMR (400 MHz, C_6D_6): δ = 7.35 (s, 1H), 6.16 (s, 1H), 5.10 (m, 2H), 4.67 (s, 2H), 4.48 (s, 2H), 1.15 ppm (m, 6H); ^{13}C NMR (100 MHz, C_6D_6): δ = 162.87, 148.86, 148.82, 137.11, 116.33, 116.16, 115.11, 82.67, 82.65, 81.07, 23.79, 23.66 ppm; HRMS-ESI: *m/z*: calcd for $C_{14}H_{14}NaO_2$: 237.0891; found: 237.0894 [$M+Na^+$].

3,6-Dimethylene-1,8-dihydrofuro[3,4-*e*]isobenzofuran (20): 1H NMR (400 MHz, C_6D_6): δ = 7.00 (s, 2H), 4.69 (s, 2H), 4.50 (s, 2H), 4.37 ppm (s, 4H); ^{13}C NMR (100 MHz, C_6D_6): δ = 164.05, 137.37, 136.36, 122.89, 81.39, 74.00 ppm; HRMS-ESI: *m/z*: calcd for $C_{12}H_{11}O_2$: 187.0759; found: 187.0747.

(3E,7E)-3,7-Dibenzylidene-1,5-dihydrofuro[3,4-*f*]isobenzofuran (30):

1H NMR (400 MHz, $[D_{10}]$ -*o*-xylene): δ = 7.41 (s, 2H), 7.39 (s, 2H), 7.27 (m, 4H), 7.16 (m, 4H), 6.42 (s, 2H), 5.10 (q, J = 6.3 Hz, 1H), 4.70 (s, 2H), 1.28 (d, J = 6.3 Hz, 4H); ^{13}C NMR (100 MHz, $[D_{10}]$ -*o*-xylene): δ = 163.66, 149.88, 143.79, 141.47, 137.25, 123.00, 122.82, 109.04, 108.96, 79.51 ppm; HRMS-ESI: *m/z*: calcd for $C_{24}H_{19}O_2$, 339.1385; found: 339.1373 [$M+H^+$].

(3E,7E)-3,7-Dibenzylidene-5-methyl-1,5-dihydrofuro[3,4-*f*]isobenzofuran (34):

1H NMR (400 MHz, $[D_{10}]$ -*o*-xylene): δ = 7.38 (m, 2H), 7.22 (m, 6H), 7.17 (m, 4H), 6.42 (s, 2H), 5.10 (q, J = 6.3 Hz, 1H), 4.70 (s, 2H), 1.28 (d, J = 6.3 Hz, 3H); ^{13}C NMR (100 MHz, $[D_{10}]$ -*o*-xylene): δ = 163.20, 162.13, 152.10, 147.68, 144.68, 144.36, 144.20, 143.68, 134.15, 119.98, 119.69, 105.22, 105.04, 89.26, 81.70, 29.01 ppm; HRMS-ESI: *m/z*: calcd for $C_{25}H_{21}O_2$: 353.1542; found: 353.1552 [$M+H^+$].

(1E,5E)-1,5-Dibenzylidene-3,7-dimethyl-3,7-dihydrofuro[3,4-*f*]isobenzofuran (36):

1H NMR (400 MHz, $[D_{10}]$ -*o*-xylene): δ = 7.34 (m, 4H), 7.22 (m, 6H), 7.13 (m, 2H), 6.33 (s, 2H), 5.12 (m, 2H), 1.28 ppm (m, 6H); ^{13}C NMR (100 MHz, $[D_{10}]$ -*o*-xylene): δ = 162.15, 152.33, 144.32, 141.50, 134.12, 123.03, 119.86, 108.88, 105.10, 89.30, 29.01 ppm; HRMS-ESI: *m/z*: calcd for $C_{26}H_{22}NaO_2$: 389.1517; found: 389.1518 [$M+Na^+$].

(1E,7E)-1,7-Dibenzylidene-3,5-dihydrofuro[3,4-*f*]isobenzofuran (38):

1H NMR (400 MHz, $[D_{10}]$ -*o*-xylene): δ = 8.05 (m, 2H), 7.49 (m, 6H), 7.21 (m, 4H), 6.06 (s, 2H), 4.97 ppm (s, 4H); ^{13}C NMR (100 MHz, $[D_{10}]$ -*o*-xylene): δ = 162.98, 147.96, 143.97, 140.89, 139.19, 135.09, 121.32, 121.23, 108.83, 105.08, 81.64 ppm; HRMS-ESI: *m/z*: calcd for $C_{48}H_{36}NaO_4$: 699.2511; found: 699.2506 [$2M+Na^+$].

(1E,7E)-1,7-Dibenzylidene-3,5-dimethyl-3,5-dihydrofuro[3,4-*f*]isobenzofuran (40):

1H NMR (400 MHz, $[D_{10}]$ -*o*-xylene): δ = 8.17 (s, 1H), 7.63 (s, 1H), 7.33 (m, 4H), 7.16 (m, 6H), 6.41 (s, 2H), 5.26 (m, 2H), 1.39 ppm (m, 6H); ^{13}C NMR (100 MHz, $[D_{10}]$ -*o*-xylene): δ = 162.15, 156.22, 152.85, 142.76, 137.30, 134.24, 121.20, 121.02, 109.34, 104.55, 86.20, 28.96 ppm; HRMS-ESI: *m/z*: calcd for $C_{26}H_{22}NaO_2$: 389.1517; found: 389.1528 [$M+Na^+$].

(3E,6E)-3,6-Dibenzylidene-1,8-dihydrofuro[3,4-*e*]isobenzofuran (42):

1H NMR (400 MHz, $[D_{10}]$ -*o*-xylene): δ = 7.98 (s, 2H), 7.48 (m, 3H), 7.38 (m, 3H), 7.29 (m, 2H), 7.20 (m, 2H), 6.03 (s, 2H), 4.70 ppm (s, 4H); ^{13}C NMR (100 MHz, $[D_{10}]$ -*o*-xylene): δ = 163.17, 145.24, 144.15, 139.37, 137.06, 133.94, 128.28, 127.37, 107.92, 105.44, 80.14 ppm; HRMS-ESI: *m/z*: calcd for $C_{24}H_{19}O_2$: 339.1385; found: 339.1388 [$M+H^+$].

Kinetic studies of hydroalkoxylation/cyclization: In a typical experiment, an NMR sample was prepared as described above (see Typical NMR-

Scale Catalytic Reactions) but maintained at -78°C until kinetic measurements were begun. The sample tube was inserted into the probe of the INOVA-400 spectrometer which had been previously set to the desired temperature ($T \pm 0.1^{\circ}\text{C}$; checked with a methanol or ethylene glycol temperature standard). A single acquisition ($\text{nt}=1$) with a 45° pulse was used during data acquisition to avoid saturation. The data were processed with the SigmaPlot 2002 program.^[43] The product concentration was measured from the area of the olefinic peak *cis* to oxygen, A_s , standardized to A_b , the methyl peak area of the free $\text{NH}(\text{SiMe}_3)_2$ formed as turnover commenced. The turnover frequency, $N_t (\text{h}^{-1})$, was calculated from the least-squares determined slope (m) according to Equation (8), where $[\text{catalyst}]_0$ is the initial concentration of the precatalyst. As determined from the least-square analysis, the uncertainty in N_t values is on the order of 2–8%.

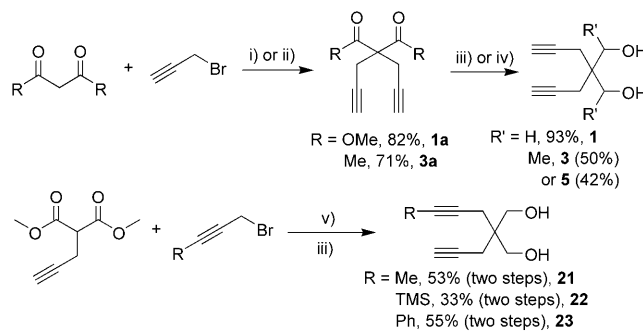
$$[\text{product}] = mt \quad (8)$$

$$N_t (\text{h}^{-1}) = \frac{60\text{min}}{\text{h}} \times \frac{m}{[\text{catalyst}]_0} \quad (9)$$

Results

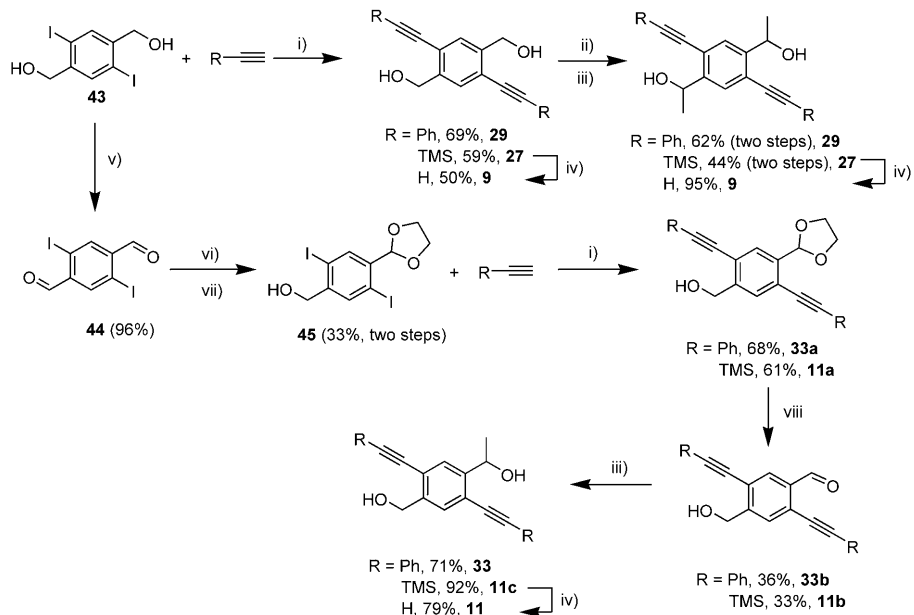
The principal goal of this contribution is to explore the scope and selectivity of the lanthanide-mediated intramolecular tandem double hydroalkoxylation/cyclization of dialkynyl dialcohols, in search of general, highly stereoselective catalytic pathways for diheterocycle construction. This section first presents synthetic routes to the various dialkynyl dialcohol substrates. Second, the effects of varying substrate substituents on the intramolecular tandem double hydroalkoxylation/cyclizations are explored, including the rates and stereochemistry of transformations involving terminal dialkynyl dialcohols versus internal dialkynyl dialcohols. Third, metal effects on the course and rates of catalytic intramolecular tandem double hydroalkoxylation/cyclizations of the various alkynyl alcohol substrates are described. Finally, the reaction kinetics and plausible mechanistic pathways are discussed, including rate laws, activation parameters, kinetic isotope effects, and their mechanistic implications.

Substrate synthesis:^[44] To explore the effects of the various substrates on lanthanide complex-mediated tandem C–O bond forming reactivity and selectivity, a number of new dialkynyl dialcohols were synthesized and characterized. Compounds **1**, **3**, **5**, **21**, **22** and **23** were synthesized by adapting published procedures, as outlined in Scheme 2.^[39] Addition



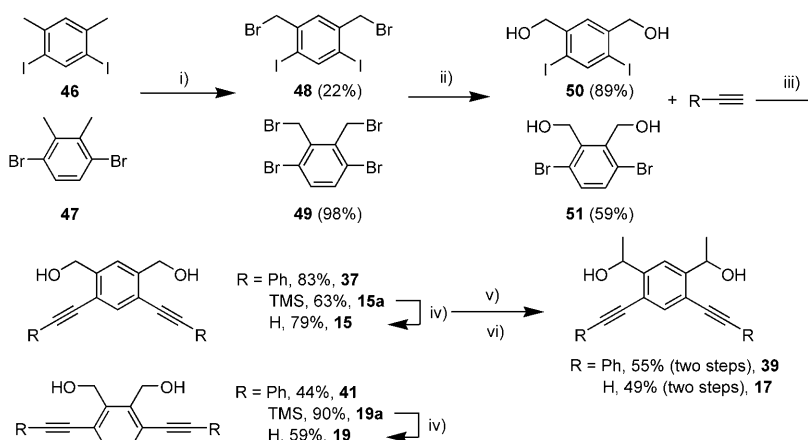
Scheme 2. Synthesis of 1,3-propanediol derivatives. i) NaOEt , EtOH , RT, 12 h; ii) K_2CO_3 , TBAHS, CH_3CN , reflux, 12 h; iii) LiAlH_4 , Et_2O , reflux, 3 h; iv) NaBH_4 , MeOH , RT, 1 h; v) NaH , THF , reflux, 12 h. TBAHS = *tert*-butylammonium hydrogensulfate.

of propargyl bromide or substituted propargyl bromides to the commercially available dimethyl malonate, acetyl acetone, or dimethyl propargylmalonate, followed by reduction using LiAlH_4 or NaBH_4 , affords each substrate in good yield. A synthetic scheme for *para*-substituted alcohols **9**, **11**, **13**, **27**, **29**, **33** and **35** is summarized in Scheme 3. Thus, substrates **9**, **13**, **27**, **29** and **35** were synthesized via Sonogashira coupling and oxidation, followed by addition of the Grignard reagent derived from compound **43**, according to published procedures.^[45] Substrates **11** and **33** were obtained by oxidation to the corresponding aldehydes, mono acetal protection, reduction, Sonogashira coupling, deprotection of the acetal, and then Grignard reaction. A synthetic scheme for *meta*- and *ortho*-substituted dialcohols **15**, **17**, **19**, **37**, **39** and **41** is summarized in Scheme 4. Compounds **50** and **51** can be obtained from compounds **46**^[46] and **47**^[47] by benzylic



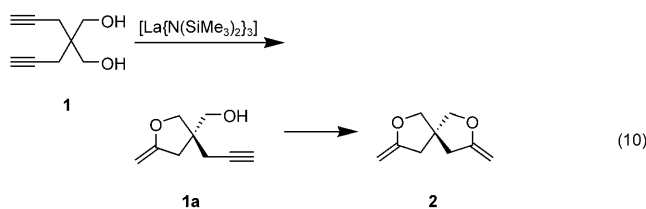
Scheme 3. Synthesis of *para*-substituted diol derivatives. i) $[\text{Pd}(\text{PPh}_3)_4]$, CuI , TEA, 50°C , 5 h; ii) $(\text{COCl})_2$, DMSO , TEA, CH_2Cl_2 , -78°C to RT, 12 h; iii) MeMgBr , THF , reflux, 2 h; iv) TBAF , THF , RT, 2 h; v) PCC , 4 Å molecular sieves, CH_2Cl_2 , reflux, 5 h; vi) ethylene glycol, TsOH , toluene, reflux, 2 h; vii) NaBH_4 , MeOH , RT, 2 h; viii) PPTS, acetone/ H_2O 2:1, reflux, 12 h.

bromination using NBS and a radical initiator, followed by hydrolysis according to published procedures. Sonogashira coupling is then conducted to afford the substrates **15**, **19**, **37** and **41**. Compounds **17** and **39** can be synthesized through Swern oxidation to corresponding aldehydes, followed by Grignard methylation. Unfortunately, the same reaction sequence applied to **19** and **41** does not yield the expected products.



Scheme 4. Synthesis of *meta*- and *ortho*-substituted diol derivatives. i) NBS, cat. BPO, CCl_4 , reflux, 12 h; ii) CaCO_3 , dioxane/ H_2O 2:1, reflux, 12 h; iii) $[\text{Pd}(\text{PPh}_3)_4]$, CuI , TEA, 50°C , 5 h; iv) TBAF, THF, RT, 2 h; v) $(\text{COCl})_2$, DMSO, TEA, CH_2Cl_2 , -78°C to RT, 12 h; vi) MeMgBr , THF, reflux, 2 h. NBS = *N*-bromosuccinimide, BPO = benzoyl peroxide.

Scope of terminal dialkynyl dialcohol catalytic intramolecular hydroalkoxylation/cyclization: The homoleptic $[\text{Ln}(\text{N}(\text{SiMe}_3)_2)_3]$ lanthanide amido complexes serve as effective precatalysts for the clean and, in most cases, quantitative tandem double intramolecular hydroalkoxylation/cyclization of a variety of selected terminal dialkynyl dialcohols to yield the corresponding spirofuran and isobenzofuran heterocycles as summarized in Table 1, where N_t is the catalytic turnover frequency for final product formation at the temperature indicated. In general, the catalytic tandem double intramolecular hydroalkoxylation/cyclization reactions of the terminal dialkynyl dialcohols examined proceed to completion at $70\text{--}120^\circ\text{C}$ under inert atmosphere, at 5 mol % catalyst loading in 1 to 12 h. In the present study, the homoleptic lanthanide amides, $[\text{Ln}(\text{N}(\text{SiMe}_3)_2)_3]$ are found by ^1H NMR spectroscopy to undergo essentially instantaneous $\text{Ln}-\text{N}$ bond protonolysis by the dialkynyl dialcohols at room temperature to yield the corresponding alkoxides and free $\text{HN}(\text{SiMe}_3)_2$. In regard to reaction sequence, *in situ* ^1H NMR spectroscopy indicates that at 120°C with 5 mol % $[\text{La}(\text{N}(\text{SiMe}_3)_2)_3]$ as the precatalyst, the dialkynyl alcohol substrates first undergo conversion to monocyclized intermediates on essentially the same time scale as the intermediates then undergo conversion to the final products [e.g., Eq. (10), Figure 1]. At the conclusion of turnover, only the bicyclic products are observed in this tandem double hydroalkoxylation/cyclization. Quantitative aspects of the reaction progress are conveniently monitored from intensity changes in the product olefinic resonances by ^1H NMR spectroscopy,



using the evolved $\text{HN}(\text{SiMe}_3)_2$ signals as an internal standard (e.g., Figure 1). Turnover frequencies were determined in $[\text{D}_{10}]\text{-}o\text{-xylene}$ or $[\text{D}_6]\text{-benzene}$ solutions from the slope of the kinetic plots of the [product]/[catalyst] ratio versus time. During the course of reactions, the monocyclized intermediates are generally observed in the ^1H NMR spectra except in the case of the very rapid conversions (Table 1, entries 5, 6, and 7). The final spirofuran and isobenzofuran products can be straightforwardly purified by column chromatography or vacuum transfer, and were characterized by ^1H , ^{13}C NMR spectroscopy, and either high-resolution MS or elemental analysis (see the Experimental Section for details).

It can be seen in Table 1 that the anaerobic cyclization of the diverse series of dialkynyl dialcohols, mediated by the homoleptic $[\text{La}(\text{N}(\text{SiMe}_3)_2)_3]$ precatalyst, proceeds with near-quantitative conversions and reasonably rapid turnover frequencies at $70\text{--}120^\circ\text{C}$. The reaction scope was designed to probe a variety of structural effects on this catalytic transformation, including five-membered ring formation using a variety of primary and secondary alcohols. It is found that spirofurans (Table 1, entries 1–3) and isobenzofurans (Table 1, entries 6–11) are cleanly formed via 5-*exo* cyclization and that there is no NMR spectroscopic evidence for the alternative 6-*endo* cyclization products [e.g., Eq. (11)]. As observed for the organolanthanide-mediated hydroalkoxylation/cyclization of simple alkynyl alcohols,^[33b] arene-substituted alcohol cyclization rates are somewhat more rapid than those for linear alcohols. Thus, the overall **15** → **16** and **19** → **20** transformations are significantly more rapid than **1** → **2** ($N_t=5.8, 6.1 \text{ h}^{-1}$ at 70°C vs. 3.9 h^{-1} at 120°C). The secondary alkynyl alcohol cases raise interesting questions about structural effects governing cyclization rates. For the aromatic substrates, the presence of a secondary alkynyl alcohol enhances the cyclization rates; thus, **17** → **18** is more

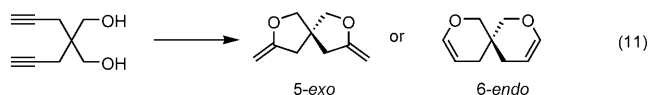


Table 1. Catalytic lanthanide-mediated tandem double intramolecular hydroalkoxylation/cyclization of alkyne-terminal dialkynyl dialcohols.

| Entry | Substrate | Product ^[a] | N_t [h ⁻¹] ([°C]) ^[b] |
|-------|-----------|------------------------|--|
| 1 | 1 | 2 | 3.9 (120) ^[c] |
| 2 | meso 3 | meso 4 | 6.8 (120) ^[c] |
| 3 | d/l 5 | d/l 6 | 7.4 (120) ^[c] |
| 4 | 7 | 8 | decomposed ^[d] |
| 5 | 9 | 10 | >1000 ^[e] |
| 6 | 11 | 12 | >1000 ^[e] |
| 7 | 13 | 14 | >1000 ^[e] |
| 8 | 15 | 16 | 5.8 (70) |
| 9 | 17 | 18 | 7.2 (70) |
| 10 | 19 | 20 | 6.1 (70) |

[a] Yields ≥95% by ¹H NMR spectroscopy and GC/MS. [b] Turnover frequencies measured in [D₆]-benzene with 5 mol % [La{N(SiMe₃)₂}₃] precatalyst. [c] Turnover frequencies measured in [D₁₀]-*o*-xylene with 5 precatalyst mol %. [d] Decomposed at 120°C over the course 4 d. [e] N_t > 1000=too fast to determine the turnover frequency.

rapid than **15**→**16** (N_t =7.2 vs. 5.8 h⁻¹ at 70°C). For linear secondary dialkynyl dialcohols, the cyclization rate is also increased; thus, the **3**→**4** and **5**→**6** transformations are significantly more rapid than **1**→**2** (N_t =6.8, 7.4 h⁻¹ vs. 3.9 h⁻¹ at 120°C). However, this trend for linear alkynyl alcohols is opposite that in single hydroalkoxylation/cyclizations. Another interesting observation concerning this transformation is that the diastereomers **3** and **5** exhibit very similar cyclization rates. This result suggests that future diastereomeric substrates can be used as mixtures of *d/l* and *meso* isomers.

The arene-substituted dialcohols can be categorized as *ortho*, *meta* and *para* substrates according to the alcohol position. The alcohol positional dependence of cyclization rates (N_t) for these substrates is pronounced: *para*>*ortho*>*meta* (N_t =>1000, 6.1, 5.8 h⁻¹ at 70°C, respectively).

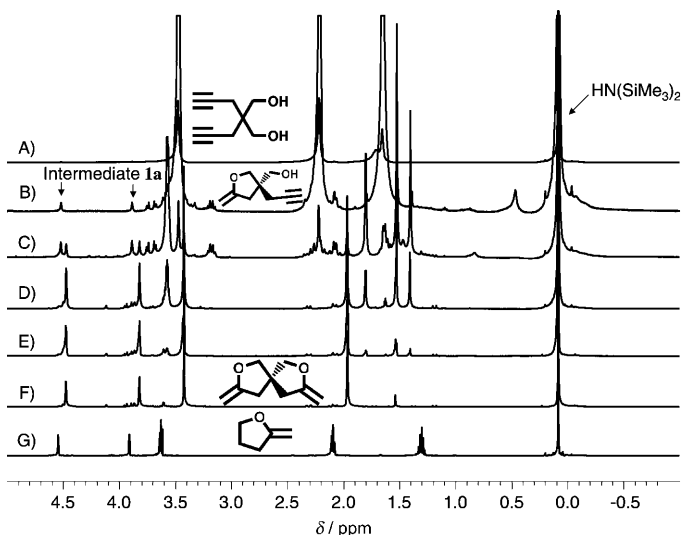


Figure 1. ¹H NMR monitoring (500 MHz) of the cyclization **1**→**2** mediated by a [La{N(SiMe₃)₂}₃] precatalyst in C₆D₆. A) $t=0.0$ h at 25°C, B) $t=1.0$ h at 90°C, C) $t=40$ min at 120°C, D) $t=2.0$ h at 120°C, E) $t=4.0$ h at 120°C, F) $t=9.0$ h at 120°C, and G) authentic methylenetetrahydrofuran sample for reference.

Stereoselectivity issues for hydroalkoxylation/cyclization of internal dialkynyl dialcohols: The intramolecular hydroalkoxylation/cyclization of alkyne-internal dialkynyl dialcohols mediated by the homoleptic [Ln{N(SiMe₃)₂}₃] lanthanide amido precatalysts proceeds effectively and selectively to yield the corresponding isobenzofurans, as shown in Table 2, where N_t is the measured turnover frequency for final product formation at the temperature indicated. In general, the catalytic hydroalkoxylation/cyclization reactions of the internal dialkynyl dialcohols examined proceed to completion at 120°C, with 5 mol % catalyst loading in 6 to 12 h. Reaction progress is again conveniently monitored from intensity changes in product olefinic resonances by ¹H NMR spectroscopy, using evolved HN(SiMe₃)₂ as the calibrant. Turnover frequencies were again calculated in [D₁₀]-*o*-xylene from the slopes of the kinetic plots of the [product]/[catalyst] ratio versus time. During the course of the reaction, monocyclized intermediates are again first observed in the ¹H NMR spectra. The final products were purified by column chromatography or vacuum transferred with other volatiles and characterized by ¹H, ¹³C NMR spectroscopy, NOESY, and high-resolution MS or elemental analysis (see the Experimental Section). According to the previous mechanistic results for internal monoalcohol hydroalkoxylation/cyclization (Scheme 1), the stereochemistry of the principal products is expected to be the *E* conformer. Indeed, the actual stereochemistry in the present transformations is confirmed to be the *E* conformers in each case by NOESY experiments.

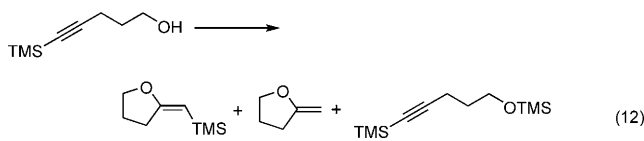
The scope of the present organolanthanide-mediated hydroalkoxylation/cyclizations of alkyne-internal dialkynyl dialcohols is summarized in Table 2. Under identical reaction conditions, the cyclization rates of the alkyne-internal dialkynyl dialcohols (Table 2) are significantly slower than

Table 2. Lanthanide-mediated catalytic intramolecular hydroalkoxylation/cyclization of alkyne-internal dialkynyl dialcohols.

| Entry | Substrate | Product ^[a] | N_t [h ⁻¹] ([°C]) ^[b] |
|-------|-----------|------------------------|--|
| 1 | | | traces (120) ^[c] |
| 2 | | | product mixture (120) ^[d] |
| 3 | | | 1.8 (120) |
| 4 | | | 2.2 (120) |
| 5 | | | 4.4 (120) |
| 6 | | | 5.8 (120) |
| 7 | | | 0.31 (120) |
| 8 | | | 1.09 (120) |
| 9 | | | 0.66 (120) |

[a] Yields $\geq 95\%$ by ¹H NMR spectroscopy and GC/MS. [b] Turnover frequencies measured in [D₁₀]-*o*-xylene with 5 mol % [La(N(SiMe₃)₂)₃] precatalyst. [c] Traces = $\approx 5\%$ completion after one week. [d] Product mixture = products too numerous to accurately determine the turnover frequency.

those of the corresponding alkyne-terminal dialkynyl dialcohols (Table 1). For linear alkyne-internal dialkynyl dialcohols (Table 2, entry 1), hydroalkoxylation/cyclizations are extremely sluggish in comparison to the alkyne-terminal substrates. The substrate having an SiMe₃-terminated alkynyl alcohol (Table 2, entry 2) is observed to yield multiple products as judged by ¹H NMR spectroscopy and is reminiscent of our previous findings that hydroalkoxylation/cyclization of the SiMe₃-terminated internal alkynyl alcohols reveals interesting product profiles which include the desired exocyclic ether, a SiMe₃-eliminated exocyclic ether, and the Me₃Si-O-functionalized substrate [Eq. (12)].^[33b] Secondary aromatic dialkynyl dialcohols undergo cyclizations at en-

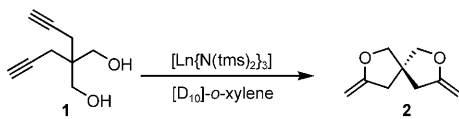


hanced rates; thus, the **33**→**34** and **35**→**36** transformations are significantly more rapid than **29**→**30** ($N_t = 4.4, 5.8 \text{ h}^{-1}$ vs. 1.8 h^{-1} at 120°C), and the **39**→**40** transformation is significantly more rapid than **37**→**38** ($N_t = 1.09 \text{ h}^{-1}$ vs. 0.31 h^{-1} at 120°C). The arene-substituted substrates can be categorized as *ortho*, *meta* and *para* according to the alcohol positions, and the alcohol positional dependence of the cyclization rates (N_t) for these substrates is significantly less than for the terminal alkynyl substrates discussed above: *para*>*ortho*>*meta* ($N_t = 1.8, 0.66, 0.31 \text{ h}^{-1}$ at 120°C , respectively).

Metal ion effects on catalytic dialkynyl dialcohol hydroalkoxylation/cyclization: In the case of catalytic aminoalkene hydroamination/cyclization, both increasing the Ln³⁺ ionic radius and opening the lanthanocene coordination sphere by *ansa*-fusion of the ancillary ligands^[48] increases the observed turnover frequencies (N_t), presumably reflecting the significant steric demands in the olefinic insertive transition state. In contrast, an approximately opposite ionic radius– N_t trend is observed for less sterically demanding aminoalkyne hydroamination/cyclization where smaller Ln³⁺ ions permit closer N–C bond-forming approach in the transition state.^[19a,j] These basic mechanistic scenarios are supported by DFT level quantum chemical computation.^[32a,b] Interestingly, our previous non-lanthanocene catalytic intramolecular alkynyl alcohol hydroalkoxylation/cyclization results (Scheme 1) exhibit kinetic trends similar to those in the aforementioned aminoalkene hydroamination/cyclization. Catalyst structural effects qualitatively similar to those in aminoalkene hydroamination/cyclization and alkynyl alcohol hydroalkoxylation/cyclization are also operative in the present bicyclization systems. Thus, for the representative cyclization **1**→**2**, Table 3 shows that the measured N_t values for **2** formation increase substantially with increasing metal ionic radius.^[49] That is, these tandem double hydroalkoxylation/cyclizations of dialkynyl dialcohols experiences similar appreciable acceleration in rate when larger ionic radius Ln³⁺ catalysts are introduced, and the kinetic and other data argue that the turnover-limiting step is C=C insertion into the Ln–O bond (Scheme 1, step i) as will be discussed in more detail below.

Kinetic and mechanistic analysis of dialkynyl dialcohol hydroalkoxylation/cyclization: Quantitative kinetic studies of representative cyclization **1**→**2** were carried out with 2.5–20.0 mol % precatalyst in [D₁₀]-*o*-xylene at 120°C by ¹H NMR spectroscopic monitoring. The evolution of specific olefinic resonances (shown in Figure 1; either that at $\delta \approx 3.7$ or at 4.5 ppm) was monitored by ¹H NMR spectroscopy and integrated versus NH(SiMe₃)₂, which is immediately and stoichiometrically generated upon substrate addition (Figure 1). Cyclizations were performed with a 10–90 fold

Table 3. Effect of varying lanthanide ionic radius on turnover frequencies in catalytic dialkynyl dialcohol intramolecular hydroalkoxylation/cyclization.



| Entry | Ln | Ionic radius [\AA] | $N_t [\text{h}^{-1}] (\text{^\circ C})^{[a]}$ |
|-------|----|-------------------------------|---|
| 1 | La | 1.160 | 3.9 (120) |
| 2 | Nd | 1.109 | 3.7 (120) |
| 3 | Sm | 1.079 | 2.3 (120) |
| 4 | Y | 1.019 | 0.63 (120) |
| 5 | Lu | 0.977 | 1.9 (120) |

[a] Turnover frequencies for product **2** formation measured in $[\text{D}_{10}]\text{-o-xylene}$ with 5 mol % precatalyst.

molar excess of substrate over catalyst, and in all cases substrate was completely consumed by the end of the reaction. In the present study, the linear increase of bicycized product **2** with conversion time suggests zero-order dependence while the decrease of substrate **1** with time shows deviations from the zero-order linearity (depressed rates) after about the first half-life (Figure 2). This deviation can be modeled by competitive product or intermediate inhibition of the conversion.^[19d,l,n,50] Since this kinetic plot can be fit very well over a broad range of conversions with an exponential curve (Figure 2), it is not straightforward to distinguish between zero-order kinetics with substantial competitive product or intermediate inhibition and real first-order kinetics by the integrated rate law method alone. Therefore, the half-life method in conjunction with the initial rate method^[51] was employed to estimate the reaction order in dialkynyl dialcohol substrate concentration for transformation **1**→**2** using 5 mol % $[\text{La}(\text{N}(\text{SiMe}_3)_2)_3]$ as the precatalyst. Three reactions starting with different initial substrate concentrations were analyzed by ^1H NMR spectroscopy. Instead of actual half-life points for each run, projected half-life points from the first 20% conversion data were determined and plotted

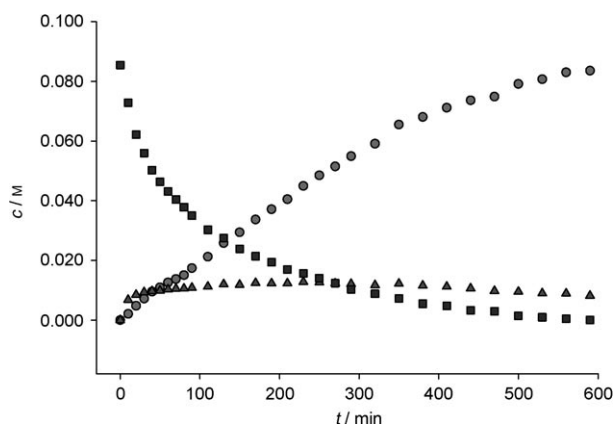


Figure 2. Concentration of substrate 2,2-di(prop-2-ynyl)propane-1,3-diol (**1**, ■), intermediate (5-methylene-3-(prop-2-ynyl)-tetrahydrofuran-3-yl)-methanol (**1a**, △), and product 3,8-dimethylene-2,7-dioxaspiro[4.4]nonane (**2**, ○) as a function of time for the hydroalkoxylation/cyclization of **1** using 5.0 mol % $[\text{La}(\text{N}(\text{SiMe}_3)_2)_3]$ as the precatalyst in $[\text{D}_{10}]\text{-o-xylene}$ at 120°C .

versus initial substrate concentration because of possible product participation influence on the reaction rate. Figure 3a shows that the half-life points increase linearly with initial substrate concentration, clearly indicating zero-order kinetics in [substrate] [Eqs. (13), (14)].

$$\frac{-d[S]}{dt} = k [S]^n \quad (13)$$

$$n=0 : [S]_t = [S]_0 - kt \quad t_{1/2} = \frac{[S]_0}{2k} \quad (14)$$

$$n=1 : [S]_t = [S]_0 e^{-kt} \quad t_{1/2} = \frac{\ln 2}{k} \quad (15)$$

$$\text{in general } (n \neq 1), \quad t_{1/2} = \frac{(2^{n-1}-1)}{k(n-1)[S]_0^{n-1}} \quad (16)$$

$$\ln t_{1/2} = \ln \frac{(2^{n-1}-1)}{k(n-1)} + (1-n) \ln [S]_0 \quad (17)$$

Modified general Equation (17) shows that the slope of the line equals $1-n$ (n =reaction order). Figure 3b also indicates zero-order kinetics in [substrate]. Therefore, the observed deviation from linearity likely reflects product or intermediate participation. Further discussion of these mechan-

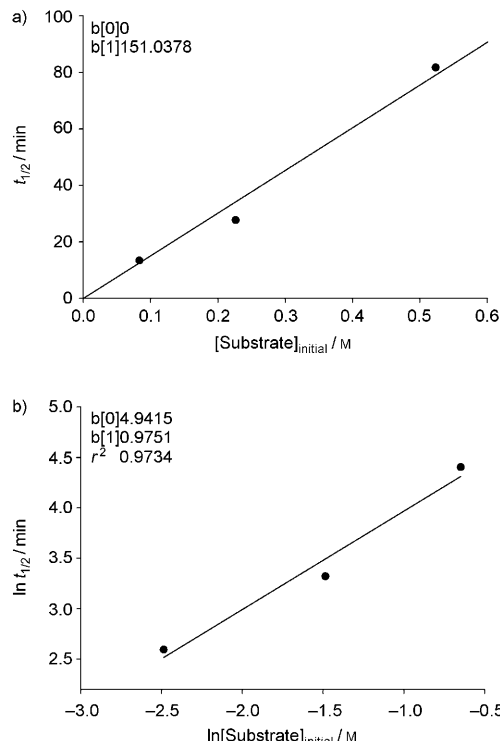


Figure 3. a) Plot of half-life points projected from the initial 20% conversion as a function of initial substrate concentration for the hydroalkoxylation/cyclization of 2,2-di(prop-2-ynyl)propane-1,3-diol (**1**) using the precatalyst $[\text{La}(\text{N}(\text{SiMe}_3)_2)_3]$ in $[\text{D}_{10}]\text{-o-xylene}$ at 120°C . The line is the least-squares fit to the data points with y intercept 0.0. b) Half-life method plot for the hydroalkoxylation/cyclization of 2,2-di(prop-2-ynyl)propane-1,3-diol (**1**) using the precatalyst $[\text{La}(\text{N}(\text{SiMe}_3)_2)_3]$ in $[\text{D}_{10}]\text{-o-xylene}$ at 120°C . The line is the least-squares fit to the data points. The $b[0]$ and $b[1]$ denote the intercept and slope of each plot, respectively.

nistic implications is deferred to the Discussion Section. When the initial concentration of dialkynyl dialcohol is held constant, and the concentration of precatalyst is varied over 10-fold range, a plot of the reaction rate of **2** formation from **1a** versus precatalyst concentration (Figure 4a) and a plot of $\ln(\text{rate})$ versus $\ln([\text{catalyst}])$ (van 't Hoff plot, slope = reaction order, Figure 4b) indicate the rate law to be the first-order in [catalyst]. Overall, the empirical rate law can be expressed as in Equation (18) and is identical to that determined for organolanthanide-catalyzed aminoalkene hydroamination/cyclization^[19] and monoalkyne monoalcohol hydroalkoxylation/cyclization.^[33]

$$\text{rate} = k[\text{substrate}]^0[\text{catalyst}]^1 \quad (18)$$

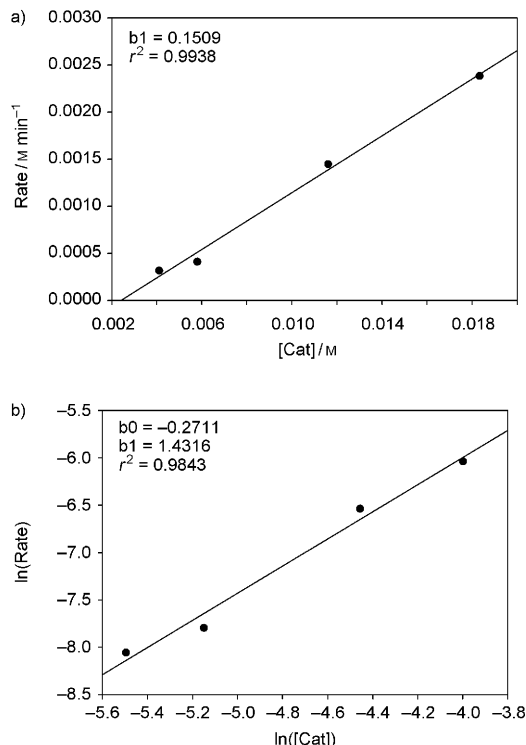


Figure 4. a) Determination of the reaction order in lanthanide concentration for the hydroalkoxylation/cyclization of 2,2-di(prop-2-ynyl)propane-1,3-diol (**1**) to 3,8-dimethylene-2,7-dioxaspiro[4.4]nonane (**2**) using the $[\text{La}(\text{N}(\text{SiMe}_3)_2)_3]$ precatalyst in $[\text{D}_{10}]\text{-o-xylene}$ at 120°C . b) van 't Hoff plot of the hydroalkoxylation/cyclization of 2,2-di(prop-2-ynyl)propane-1,3-diol (**1**) using $[\text{La}(\text{N}(\text{SiMe}_3)_2)_3]$ as the precatalyst in $[\text{D}_{10}]\text{-o-xylene}$ at 120°C . The lines are least-squares fits to the data points. The $b[0]$ and $b[1]$ denote the intercept and slope of each plot, respectively.

Variable-temperature kinetic studies were conducted by *in situ* ^1H NMR spectroscopy for the rate of **2** formation mediated by $[\text{La}(\text{N}(\text{SiMe}_3)_2)_3]$. Data are shown in Figure 5a normalized to the free $\text{NH}(\text{SiMe}_3)_2$ concentration. The rate of **2** formation mediated by $[\text{La}(\text{N}(\text{SiMe}_3)_2)_3]$ is independent of substrate concentration over a 30°C temperature range ($100\text{--}130^\circ\text{C}$), suggesting zero-order dependence on substrate concentration, in accord with the kinetic results discussed above. Standard Eyring (Figure 5b) and Arrhenius (Fig-

ure 5c) kinetic analyses^[52] yield activation parameters $\Delta H^\ddagger = 17.5(1.4)$ kcal mol⁻¹, $\Delta S^\ddagger = -29.9(3.5)$ e.u., and $E_a = 18.2(1.4)$ kcal mol⁻¹.^[53] Furthermore, an -OH versus -OD isotopic labeling study (Table 2, entry 4), assayed by ^1H and ^2H NMR spectroscopy of product formation, yields a kinetic isotope effect (KIE) of $k_{\text{H}}/k_{\text{D}} = 0.82(0.02)$.

Discussion

Scope of catalytic intramolecular dialkynyl dialcohol hydroalkoxylation/cyclization: A central goal of this research was

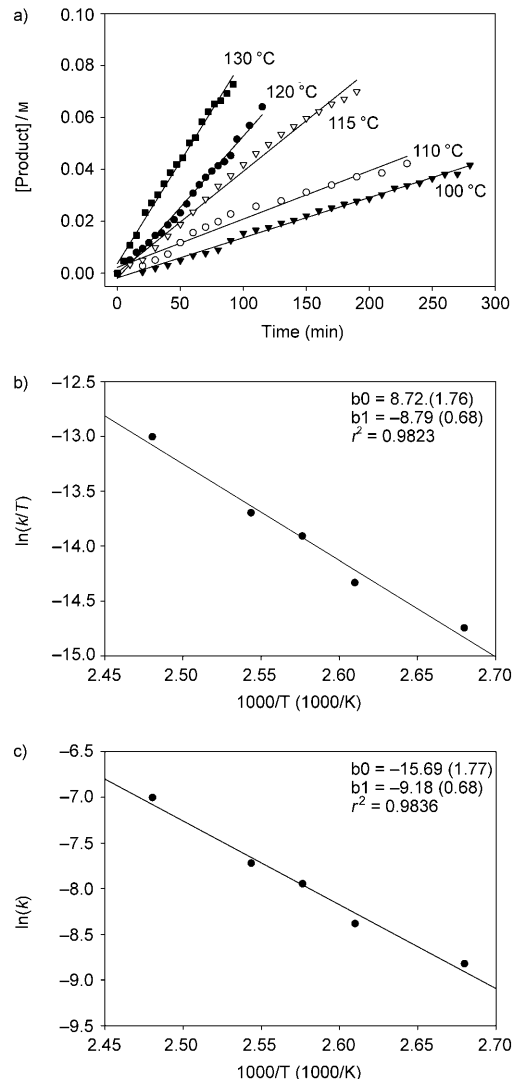


Figure 5. a) Concentration of product 2 (3,8-dimethylene-2,7-dioxaspiro[4.4]nonane) from intermediate **1a** as a function of time and temperature for the hydroalkoxylation/cyclization of 2,2-di(prop-2-ynyl)propane-1,3-diol (**1**) using 5 mol % $[\text{La}(\text{N}(\text{SiMe}_3)_2)_3]$ as the precatalyst in $[\text{D}_{10}]\text{-o-xylene}$ at various temperatures. b) Eyring plot for the intramolecular hydroalkoxylation/cyclization of **1** using $[\text{La}(\text{N}(\text{SiMe}_3)_2)_3]$ as the precatalyst in $[\text{D}_{10}]\text{-o-xylene}$. The line represents the least-squares fit to the data points. c) Arrhenius plot for the intramolecular hydroalkoxylation/cyclization of **1** using $[\text{La}(\text{N}(\text{SiMe}_3)_2)_3]$ as the precatalyst in $[\text{D}_{10}]\text{-o-xylene}$. The line represents the least-squares fit to the data points. The $b[0]$ and $b[1]$ denote the intercept and slope of each plot, respectively.

to explore the scope of homoleptic $[\text{Ln}(\text{N}(\text{SiMe}_3)_2)_3]$ lanthanide amido precatalyst-mediated tandem double intramolecular hydroalkoxylation/cyclizations of dialkynyl dialcohols. The results in Tables 1 and 2 indicate that $[\text{Ln}(\text{N}(\text{SiMe}_3)_2)_3]$ complexes are competent precatalysts for the formation of diverse five-membered ring fused diheterocycles having a variety of alkyl and aryl substituents. In the tandem double hydroalkoxylation/cyclization of both primary and secondary dialkynyl dialcohols, there is a marked difference in cyclization rates between alkyl and aromatic dialkynyl dialcohols. In general, the cyclization rates for the arene-functionalized alkynyl alcohols are more rapid than those of linear alkynyl alcohols. This may reflect configurations in

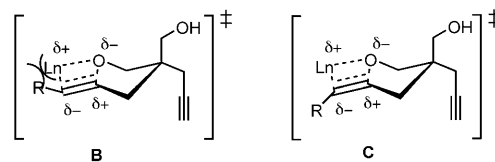
which the arene-functionalized alkynyl alcohols have more accessible, pre-organized structures than the linear alkynyl alcohols, involving interaction of the electrophilic lanthanide center with the electron-rich arene π system (e.g., A).^[54]

Comparison of the differences in primary and secondary dialkynyl dialcohol cyclization rates raises interesting questions. Specifically, the cyclization rates of the linear and arene-functionalized secondary dialkynyl dialcohols are greater than those of linear and arene-functionalized primary dialkynyl dialcohols. This suggests that among the several possible factors influencing rates, including sterics, electronics, and metal binding strength, the cyclization rates are not dominantly controlled by steric factors above all other factors. Rather, electronic factors and metal complexation effects play an important role in the cyclization rates. Note that one secondary dialkynyl dialcohol does not proceed cleanly and gives only a decomposed mixture at 120°C over four days (Table 1, entry 4).

Another instructive observation in this investigation is that these homoleptic $[\text{Ln}(\text{N}(\text{SiMe}_3)_2)_3]$ lanthanide amido precatalysts exhibit pronounced selectivity between *ortho*-, *meta*-, and *para*-substituted arene dialkynyl dialcohols (Table 1, entries 5, 8, and 10). The alcohol positional dependence of the cyclization rates for these substrates is *para* > *ortho* > *meta*. In this trend, the rapid tandem double cyclization rate of the *para*-substituted arene dialkynyl dialcohol can be explained by the lack of inhibitory coordination by a second proximate, chelating substrate alcohol ligand (A). If the selectivity derives only from the metal complexation with a second alcohol ligand of substrate, the rate of *meta*-substituted substrates should be more rapid than that of *ortho*-substituted substrates. However, the observed trend is opposite. Therefore, electronic effects also doubtless play a significant role in the transition state, suggesting a complex interplay of steric, electronic, and metal complexation energetic factors.

Stereoselectivity in alkyne-internal dialkynyl dialcohol hydroalkoxylation/cyclization: The present lanthanide-mediated hydroalkoxylation/cyclizations of alkyne-internal dialkyn-

yl dialcohols proceed with excellent stereoselectivity, and are completely *E*-selective. This high *E* selectivity can be rationalized in terms of a transition state in which the R substituents occupy the less sterically hindered positions in a chair-like cyclic transition state, similar to those proposed and identified computationally for analogous hydroamination/cyclizations,^[19,32] and monofunctional hydroalkoxylation/cyclizations^[33b] (Scheme 1; B versus C). Some explana-



tion of the R substituent effects on the cyclization reaction kinetics is also possible. Among the principal factors, the interplay of non-bonded repulsions and electronic contributions doubtless governs the hydroalkoxylation/cyclization kinetics. The fact that the cyclization rates of the alkyne-terminal alkynyl alcohols are invariably greater than those of the internal alkynyl alcohols under identical reaction conditions, and that rates increase with increasing Ln^{+3} ionic radius, argues that non-bonded repulsions dominate the first stages of the cyclization process. However, the corresponding linear alkyne-internal dialkynyl dialcohol proceeds to only $\approx 5\%$ completion at 120°C over seven days (Table 2, entry 1). This rate depression appears to reflect the interplay of R substituent steric and electronic factors. For the arene-substituted alkyne-internal substrate systems, the primary and secondary dialkynyl dialcohol cyclization rates indicate that among the several factors including sterics, electronics, and metal binding, electronic factors govern the cyclization rate. Thus, the cyclization rates of the arene-functionalized secondary dialkynyl dialcohols are substantially greater than those of arene-functionalized primary dialkynyl dialcohols similar to the case of monofunctional hydroalkoxylation/cyclization.^[33b]

The selectivity between *ortho*-, *meta*-, and *para*-substituted arene internal dialkynyl dialcohols also exhibits trends similar to those of the terminal arene-substituted substrates (Table 2, entries 3, 7, and 9). The alcohol positional dependence of the cyclization rates for these substrates is *para* > *ortho* > *meta*. This trend can be explained on the basis of interplay of the multiple factors as discussed above.

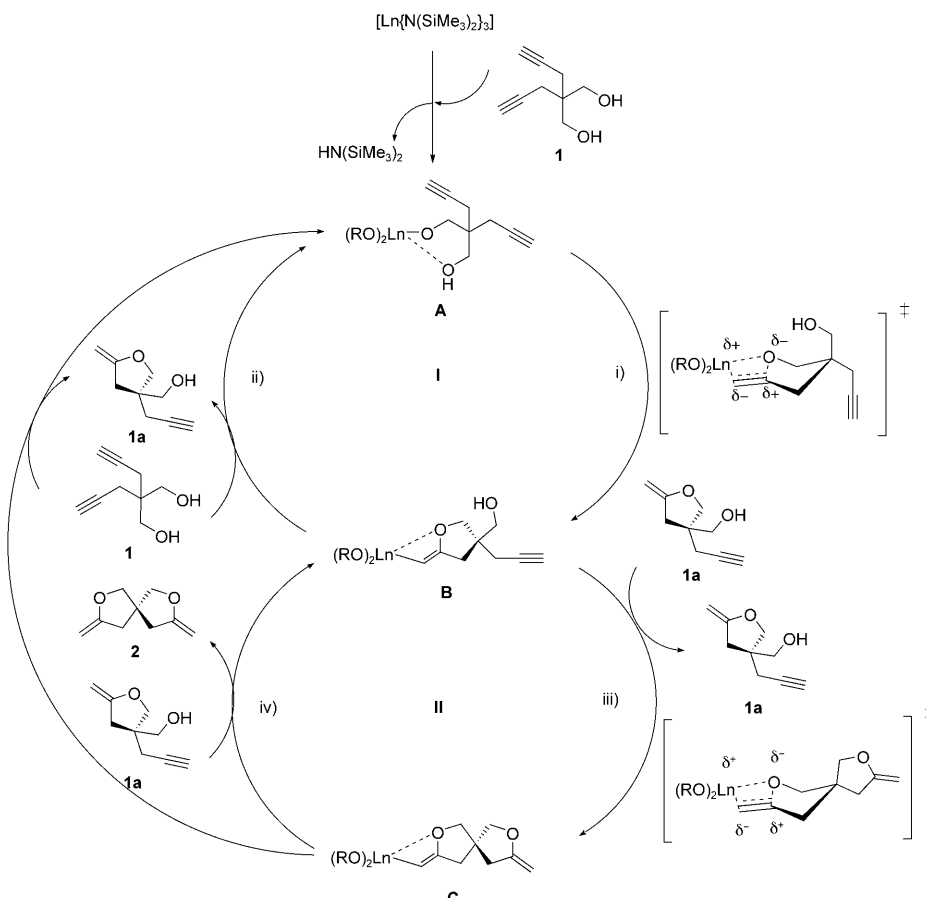
Dialkynyl dialcohol hydroalkoxylation/cyclization—kinetics and mechanism: The kinetic analysis for the **1 → 2** transformation catalyzed by $[\text{La}(\text{N}(\text{SiMe}_3)_2)_3]$ indicates essentially zero-order rate dependence on substrate concentration (Figures 2 and 3) and first-order dependence on catalyst concentration (Figure 4), similar to the scenario for lanthanocene-mediated intramolecular aminoalkene, aminoalkyne, and aminoallene hydroamination/cyclization and hydrophosphination,^[19,20,32] and monofunctional hydroalkoxylation/cycliza-

tions.^[33b] In this tandem double hydroalkoxylation/cyclization, despite the apparent kinetic similarities, a plot of substrate concentration versus time departs significantly from the typical linearity (zero-order kinetics) after about one half-life, resulting in depressed rates (seemingly first-order-like kinetic behavior, Figure 2).^[19d,l,n,50] Further investigations of this apparent first-order kinetic behavior using the half-life method in conjunction with the initial rate method reveal that the initial rate is still zero-order in substrate (Figure 3), and a kinetic plot for product formation shows the rate to be zero-order in substrate, suggesting the observed rate depression is due primarily to competitive inhibition by product and/or the reaction intermediate. It was previously observed in lanthanocene-mediated hydroamination/cyclization and hydrophosphination/cyclization that variable numbers of amine/phosphine substrate molecules are coordinated to the metal center and that these significantly modulate the diastereoselectivity of hydroelementation/cyclization as well as influence rates, mainly via competition with substrate or product molecules for the reaction centers.^[19n]

In the present tandem double hydroalkoxylation/cyclizations, the catalytic sequence as shown in Scheme 5 can be proposed. This scenario consists of two coupled cycles, **I** and **II**, which generate the monocyclized intermediate **1a** and transform it to bicycized product **2**. These two cycles raise an interesting question about the turnover-limiting step. This present results argue that two turnover-limiting steps (steps i and iii) are possible in the present case, as shown in Scheme 5. Comparison of the two plots (**1a** and **2** evolution) in Figure 2 and the olefinic peak in ¹H NMR spectrum of intermediate **1a** in Figure 1 indicate that the cycle **I** is in most cases slightly more rapid than the cycle **II**. For the conversion **1** → **2**, the half-life of **1** is about 100 min and that of **2** is about 200 min. Therefore, these half-lives also confirm this approximate rate difference. The turnover-limiting step in the present case then involves intramolecular C≡C insertion into the Ln–O bond of monocyclized product **1a** (Scheme 5, step iii), followed by rapid protonolysis of the resulting Ln–C bond (Scheme 5, step iv). This cycle would be followed by substitution via transalcoholysis to in-

duce another substrate molecule **1** or intermediate **1a** in the Ln³⁺ coordination sphere. The first-order dependence of the kinetic results on [Ln(OR)₃] also argues that the active catalyst is not in rapid pre-equilibrium with a more associated $[(\text{Ln}(\text{OR})_3)_n]^{[55]}$ species. An -OH versus -OD labeling study (Table 2, entry 4) assayed by ¹H and ²H NMR spectroscopy of product formation yields a kinetic isotope effect (KIE) of $k_{\text{H}}/k_{\text{D}} = 0.82(0.02)$, suggesting a non-primary kinetic isotopic effect, but rather a small inverse secondary kinetic isotopic effect,^[56] and consistent with the alkyne insertion being the turnover-limiting step in the catalytic cycle.

The present activation parameters for transformation **1** → **2** can be compared to the corresponding parameters for the hydroamination/cyclization of aminoalkenes, aminoalkynes, and aminoallenenes, the hydrophosphination/cyclization of a phosphinoalkene, and the single monohydroalkoxylation/cyclization of alkynyl alcohol (Table 4). In the present study, tandem double hydroalkoxylation/cyclization of an alkynyl alcohol proceeds with a modest ΔH^\ddagger and the largest negative magnitude of ΔS^\ddagger for this series of transformations (Table 4). That the tandem double alkynyl alcohol cyclization exhibits a modest enthalpic barrier and the largest magnitude of ΔS^\ddagger (more negative) implies a highly organized, polar transition state characteristic of many d⁰, fⁿ-centered



Scheme 5. Simplified proposed catalytic cycle for lanthanide-mediated tandem double intramolecular hydroalkoxylation/cyclization of dialkynyl dialcohols.

Table 4. Activation parameter comparison for intramolecular hydroamination/cyclization and hydroalkoxylation/cyclization processes.

| Entry | Substrate | Product | ΔH^\ddagger [kcal mol ⁻¹] | ΔS^\ddagger [e.u.] | E_a [kcal mol ⁻¹] |
|------------------|-----------|---------|---|----------------------------|---------------------------------|
| 1 ^[a] | | | 17.7(2.1) | -24.7(5) | 18.5(2.0) |
| 2 ^[b] | | | 16.9(1.3) | -16.5(4) | 17.6(1.4) |
| 3 ^[c] | | | 12.7(1.4) | -27.0(5) | 13.4(1.5) |
| 4 ^[d] | | | 10.7(8) | -27.4(6) | 11.3(2.0) |
| 5 ^[e] | | | 12.3(1.6) | -25.9(5.2) | 13.0(1.4) |
| 6 ^[f] | | | 20.2(1.0) | -11.8(0.3) | 20.9(0.3) |
| 7 ^[g] | | | 17.5(1.4) | -29.9(3.5) | 18.2(1.4) |

[a] Determined using $[\text{Sm}(\text{CH}(\text{SiMe}_3)_2)(\text{Me}_2\text{SiCp}'_2)]$ as the precatalyst in $[\text{D}_{10}]$ -*o*-xylene.^[19c] [b] Determined using $[\text{La}(\text{CH}(\text{SiMe}_3)_2)(\text{Cp}'_2)]$ as the precatalyst in $[\text{D}_8]$ -toluene.^[19g] [c] Determined using $[\text{La}(\text{CH}(\text{SiMe}_3)_2)(\text{Cp}'_2)]$ as the precatalyst in $[\text{D}_8]$ -toluene.^[19n] [d] Determined using $[\text{Sm}(\text{CH}(\text{SiMe}_3)_2)(\text{Cp}'_2)]$ as the precatalyst in $[\text{D}_8]$ -toluene.^[19j] [e] Determined using $[\text{Sm}(\text{CH}(\text{SiMe}_3)_2)(\text{Cp}'_2)]$ as the precatalyst in $[\text{D}_6]$ -benzene.^[20d] [f] Determined using $[\text{La}(\text{N}(\text{SiMe}_3)_2)_3]$ as the precatalyst in $[\text{D}_6]$ -benzene.^[33b] [g] Determined using $[\text{La}(\text{N}(\text{SiMe}_3)_2)_3]$ as the precatalyst in $[\text{D}_{10}]$ -*o*-xylene.

hydroelementations,^[19] and together with the large E_a^\ddagger value doubtless reflects the very large Ln–O bond enthalpies. Overall, the present results obtained from the kinetic studies (rate law, activation parameters) and from structural factors affecting cyclization rates and reaction scope (metal ion size, product ring size, substrate substituent effects) support the hydroalkoxylation/cyclization mechanistic scenario of Scheme 5,^[33] roughly analogous to, but more elaborate than, those established for hydroamination/cyclization^[19] and hydrophosphination/-cyclization,^[20] and having certain distinctive differences.

Conclusion

Tandem double intramolecular hydroalkoxylation/cyclization processes for dialkynyl dialcohol substrates mediated by homoleptic $[\text{Ln}(\text{N}(\text{SiMe}_3)_2)_3]$ lanthanide amido precatalysts exhibit a broad reaction scope in substrate type, including both alkyl and aryl primary and secondary terminal dialkynyl dialcohols and internal dialkynyl dialcohols. The present process proceeds cleanly at 70–120 °C and provides exocyclic enol ethers such as spirofurans and isobenzofurans in excellent conversion, high turnover frequencies, and regioselectivities. Mechanistic data implicate turnover-limiting insertion of C–C unsaturation into Ln–O bonds (involving a highly organized transition state) with subsequent, rapid Ln–C protonolysis.

Acknowledgements

Financial support by the NSF (Grant CHE-0809589) is gratefully acknowledged.

- [1] a) R. H. Bates, M. Chen, W. R. Roush, *Curr. Opin. Drug Discov. Devel.* **2008**, *11*, 778–792; b) K. S. M. Salih, M. T. Ayoub, H. A. Saadeh, N. A. Al-Masoudi, M. S. Mubarak, *Heterocycles* **2007**, *71*, 1577–1587; c) Y. Kashman, A. Rudi, D. Pappo, *Pure Appl. Chem.* **2007**, *79*, 491–505; d) M. C. Elliott, E. Williams, *J. Chem. Soc. Perkin Trans. 1* **2001**, 2303–2340; e) A. Mitchenson, A. Nadin, *J. Chem. Soc. Perkin Trans. 1* **2000**, 2862–2892; f) M. C. Elliott, *J. Chem. Soc. Perkin Trans. 1* **2002**, 2301–2323; g) A. J. Sargent, T. M. Cresp in *Comprehensive Organic Chemistry*, Vol. 4 (Ed.: P. G. Sammes), Pergamon, Oxford, **1979**, pp. 693–744; h) A. R. Katritzky, A. F. Pozharskii, *Handbook of Heterocyclic Chemistry*, 2nd ed., Pergamon, Oxford, **2000**.
- [2] a) Z. Zhang, C. Liu, R. E. Kinder, X. Han, H. Qian, R. A. Widenhoefer, *J. Am. Chem. Soc.* **2006**, *128*, 9066–9073; b) E. D. Cox, J. M. Cook, *Chem. Rev.* **1995**, *95*, 1797–1842; c) R. C. Larcock, W. W. Leong in *Comprehensive Organic Synthesis*, Vol. 4 (Eds.: B. M. Trost, I. Fleming), Pergamon, New York, **1991**; d) C. W. Bird, G. W. H. Cheeseman in *Comprehensive Heterocyclic Chemistry*, Vol. 4 (Eds.: A. R. Katritzky, C. W. Rees), Pergamon, Oxford, **1984**, pp. 89–154.
- [3] a) B. M. Trost, A. C. Gutierrez, R. C. Livingston, *Org. Lett.* **2009**, *11*, 2539–2542; b) F. E. McDonald, K. S. Reddy, Y. Díaz, *J. Am. Chem. Soc.* **2000**, *122*, 4304–4309; c) F. E. McDonald, *Chem. Eur. J.* **1999**, *5*, 3103–3106; d) B. M. Trost, Y. H. Rhee, *J. Am. Chem. Soc.* **1999**, *121*, 11680–11683; e) P. Compain, J. Goré, J.-M. Vatèle, *Tetrahedron* **1996**, *52*, 10405–10416; f) P. Compain, J. Goré, J.-M. Vatèle, *Tetrahedron Lett.* **1995**, *36*, 4059–4062.
- [4] a) T.-L. Ho, *Tandem Organic Reactions*, Wiley, New York, **1992**; b) L. F. Tietze, U. Beifuss, *Angew. Chem.* **1993**, *105*, 137–170; *Angew. Chem. Int. Ed. Engl.* **1993**, *32*, 131–163; c) P. A. Wender, B. L. Miller in *Organic Synthesis Theory and Applications*, Vol. 2 (Ed.: T. Hudlicky), JAI Press, Greenwich, **1993**.
- [5] For reviews on atom-economical processes, see: a) C.-J. Li, B. M. Trost, *Proc. Natl. Acad. Sci. USA* **2008**, *105*, 13197–13202; b) C. J. Li, *Chem. Rev.* **2005**, *105*, 3095–3166; c) B. M. Trost, *Acc. Chem. Res.* **2002**, *35*, 695–705; d) P. N. Anastas, M. M. Kirchhoff, *Acc. Chem. Res.* **2002**, *35*, 686–694; e) B. M. Trost, D. F. Toste, A. B. Picketton, *Chem. Rev.* **2001**, *101*, 2067–2096; f) B. M. Trost, M. J. Krische, *Synlett* **1998**, 1–16; g) B. M. Trost, *Science* **1991**, *254*, 1471–1477.
- [6] For reviews of tandem reactions, see: a) K. Hiratani, M. Albrecht, *Chem. Soc. Rev.* **2008**, *37*, 2413–2421; b) C. J. Chapman, C. G. Frost, *Synthesis* **2007**, 1–21; c) L. F. Tietze, F. Haunert, *Stimulating Concepts in Chemistry* (Eds.: F. Vögtle, J. F. Stoddart, M. Shibasaki), Wiley-VCH, Weinheim, **2000**, pp. 39–64; d) G. Poli, G. Giambastiani, A. Heumann, *Tetrahedron* **2000**, *56*, 5959–5989; e) L. F. Tietze, *Chem. Rev.* **1996**, *96*, 115–136; f) S. E. Denmark, A. Thorarensen, *Chem. Rev.* **1996**, *96*, 137–165; g) J. D. Winkler, *Chem. Rev.* **1996**, *96*, 167–176.

- [7] a) F. Alonso, I. P. Beletsaya, M. Yus, *Chem. Rev.* **2004**, *104*, 3079–3159; b) M. A. Tius in *Modern Allene Chemistry*, Vol. 2 (Eds.: N. Krause, A. S. K. Hashmi), Wiley-VCH, Weinheim, **2004**, pp. 834–838; c) K. Tani, Y. Kataoka in *Catalytic Heterofunctionalization* (Eds.: A. Togni, H. Grützmacher), Wiley-VCH, Weinheim, **2001**, pp. 171–216; d) P. A. Bartlett in *Asymmetric Synthesis*, Vol. 3 (Ed.: J. D. Morrison), Academic Press, New York, **1984**, p. 455.
- [8] For examples of alkene hydroalkoxylation, see: a) A. Dzudza, T. J. Marks, *Chem. Eur. J.* **2010**, *16*, 3403–3422; b) B. D. Kelly, J. M. Allen, R. E. Tundel, T. H. Lambert, *Org. Lett.* **2009**, *11*, 1381–1383; c) A. R. Chianese, S. J. Lee, M. R. Gagné, *Angew. Chem.* **2007**, *119*, 4118–4136; *Angew. Chem. Int. Ed.* **2007**, *46*, 4042–4059; d) L. Coulobel, M. Rajzmann, J.-M. Pons, S. Olivero, E. Duñach, *Chem. Eur. J.* **2006**, *12*, 6356–6365; e) C.-G. Yang, C. He, *J. Am. Chem. Soc.* **2005**, *127*, 6966–6967; f) Y. Oe, T. Ohta, Y. Ito, *Synlett* **2005**, 179–181; g) H. Qian, X. Han, R. A. Widenhoefer, *J. Am. Chem. Soc.* **2004**, *126*, 9536–9537.
- [9] For examples of alkyne hydroalkoxylation, see: a) S. Bhunia, K.-C. Wang, R.-S. Liu, *Angew. Chem.* **2008**, *120*, 5141–5144; *Angew. Chem. Int. Ed.* **2008**, *47*, 5063–5066; b) N. T. Patil, L. M. Lutete, H. Wu, N. K. Pahadi, I. D. Gridnev, Y. Yamamoto, *J. Org. Chem.* **2006**, *71*, 4270–4279; c) X. Li, A. R. Chianese, T. Vogel, R. H. Crabtree, *Org. Lett.* **2005**, *7*, 5437–5440; d) P. Wipf, T. H. Graham, *J. Org. Chem.* **2003**, *68*, 8798–8807; e) Y. Sheng, D. G. Musaev, K. S. Reddy, F. E. McDonald, K. Morokuma, *J. Am. Chem. Soc.* **2002**, *124*, 4149–4157; f) B. M. Trost, Y. H. Rhee, *J. Am. Chem. Soc.* **2002**, *124*, 2528–2533; g) I. Kadota, L. M. Lutete, A. Shibuya, Y. Yamamoto, *Tetrahedron Lett.* **2001**, *42*, 6207–6210; h) P. Pale, J. Chuche, *Eur. J. Org. Chem.* **2000**, 1019–1025; i) S. Elgafi, L. D. Field, B. A. Messerle, *J. Organomet. Chem.* **2000**, *607*, 97–104; j) F. E. McDonald, K. S. Reddy, Y. Díaz, *J. Am. Chem. Soc.* **2000**, *122*, 4304–4309; k) F. E. McDonald, *Chem. Eur. J.* **1999**, *5*, 3103–3106; l) D. Tzalis, C. Kordan, P. Knochel, *Tetrahedron Lett.* **1999**, *40*, 6193–6195; m) S. Cacchi, *J. Organomet. Chem.* **1999**, *576*, 42–64.
- [10] For examples of allene hydroalkoxylation, see: a) R. S. Paton, F. Maseras, *Org. Lett.* **2009**, *11*, 2237–2240; b) Z. Zhang, R. A. Widenhoefer, *Org. Lett.* **2008**, *10*, 2079–2081; c) Z. Zhang, R. A. Widenhoefer, *Angew. Chem.* **2007**, *119*, 287–289; *Angew. Chem. Int. Ed.* **2007**, *46*, 283–285; d) S. Ma, *Chem. Rev.* **2005**, *105*, 2829–2871; e) R. W. Bates, V. Satcharoen, *Chem. Soc. Rev.* **2002**, *31*, 12–21; f) C. Mukai, H. Yamashita, M. Hanaoka, *Org. Lett.* **2001**, *3*, 3385–3387.
- [11] A. Diéguez-Vázquez, C. C. Tzschucke, J. Crecente-Campo, S. McGrath, S. V. Ley, *Eur. J. Org. Chem.* **2009**, 1698–1706.
- [12] V. Belting, N. Krause, *Org. Lett.* **2006**, *8*, 4489–4492.
- [13] E. Genin, S. Antoniotti, V. Michelet, J.-P. Genêt, *Angew. Chem.* **2005**, *117*, 5029–5033; *Angew. Chem. Int. Ed.* **2005**, *44*, 4949–4953.
- [14] Y. Zhang, J. Xue, Z. Xin, Z. Xie, Y. Li, *Synlett* **2008**, 940–944.
- [15] B. A. Messerle, K. Q. Vuong, *Organometallics* **2007**, *26*, 3031–3040.
- [16] B. A. Messerle, K. Q. Vuong, *Pure Appl. Chem.* **2006**, *78*, 385–390.
- [17] A. Diéguez-Vázquez, C. C. Tzschucke, W. Y. Lam, S. V. Ley, *Angew. Chem.* **2008**, *120*, 216–219; *Angew. Chem. Int. Ed.* **2008**, *47*, 209–212.
- [18] B. Liu, J. K. De Brabander, *Org. Lett.* **2006**, *8*, 4907–4910.
- [19] a) S. Hong, T. J. Marks, *Acc. Chem. Res.* **2004**, *37*, 673–686; b) X. Yu, T. J. Marks, *Organometallics* **2007**, *26*, 365–376; c) J.-S. Ryu, T. J. Marks, F. E. McDonald, *J. Org. Chem.* **2004**, *69*, 1038–1052; d) S. Hong, A. M. Kawaoka, T. J. Marks, *J. Am. Chem. Soc.* **2003**, *125*, 15878–15892; e) J.-S. Ryu, T. J. Marks, F. E. McDonald, *Org. Lett.* **2001**, *3*, 3091–3094; f) V. M. Arredondo, S. Tian, F. E. McDonald, T. J. Marks, *J. Am. Chem. Soc.* **1999**, *121*, 3633–3639; g) V. M. Arredondo, F. E. McDonald, T. J. Marks, *J. Am. Chem. Soc.* **1998**, *120*, 4871–4872; h) Y. Li, T. J. Marks, *J. Am. Chem. Soc.* **1998**, *120*, 1757–1771; i) P. W. Roesky, C. L. Stern, T. J. Marks, *Organometallics* **1997**, *16*, 4705–4711; j) Y. Li, T. J. Marks, *J. Am. Chem. Soc.* **1996**, *118*, 9295–9306; k) Y. Li, T. J. Marks, *J. Am. Chem. Soc.* **1996**, *118*, 707–708; l) C. M. Haar, C. L. Stern, T. J. Marks, *Organometallics* **1996**, *15*, 1765; m) M. A. Giardello, V. P. Conticello, L. Brard, M. R. Gagné, T. J. Marks, *J. Am. Chem. Soc.* **1994**, *116*, 10241–10254; n) M. A. Giardello, V. P. Conticello, L. Brard, M. Sabat, A. L. Rheingold, C. L. Stern, T. J. Marks, *J. Am. Chem. Soc.* **1994**, *116*, 10212–10240; o) M. R. Gagné, C. L. Stern, T. J. Marks, *J. Am. Chem. Soc.* **1992**, *114*, 275–294.
- [20] a) A. Motta, I. L. Fragala, T. J. Marks, *Organometallics* **2005**, *24*, 4995–5003; b) A. M. Kawaoka, M. R. Douglass, T. J. Marks, *Organometallics* **2003**, *22*, 4630–4632; c) M. R. Douglass, M. Ogasawara, S. Hong, M. V. Metz, T. J. Marks, *Organometallics* **2002**, *21*, 283–292; d) M. R. Douglass, C. L. Stern, T. J. Marks, *J. Am. Chem. Soc.* **2001**, *123*, 10221–10238.
- [21] For recent organolanthanide reviews, see: a) S. B. Amin, T. J. Marks, *Angew. Chem.* **2008**, *120*, 2034–2054; *Angew. Chem. Int. Ed.* **2008**, *47*, 2006–2025; b) H. C. Aspinall, *Chem. Rev.* **2002**, *102*, 1807–1850; c) F. T. Edelmann, D. M. M. Freckmann, H. Schumann, *Chem. Rev.* **2002**, *102*, 1851–1896; d) S. Arndt, J. Okuda, *Chem. Rev.* **2002**, *102*, 1953–1976; e) G. A. Molander, A. C. Romero, *Chem. Rev.* **2002**, *102*, 2161–2186; f) M. Shibasaki, N. Yoshikawa, *Chem. Rev.* **2002**, *102*, 2187–2210; g) J. Inanaga, H. Furuno, T. Hayano, *Chem. Rev.* **2002**, *102*, 2211–2226; h) G. A. Molander, *Chemtracts: Org. Chem.* **1998**, *18*, 237–263; i) F. T. Edelmann, *Top. Curr. Chem.* **1996**, *179*, 247–276; j) F. T. Edelmann in *Comprehensive Organometallic Chemistry*, Vol. 4 (Eds.: G. Wilkinson, F. G. A. Stone, E. W. Abel), Pergamon, Oxford, **1995**, Chapter 2; k) H. Schumann, J. A. Meese-Markscheffel, L. Esser, *Chem. Rev.* **1995**, *95*, 865–986; l) T. J. Marks, R. D. Ernst in *Comprehensive Organometallic Chemistry* (Eds.: G. Wilkinson, F. G. A. Stone, E. W. Abel), Pergamon, Oxford, **1982**, Chapter 21.
- [22] a) S. A. Schuetz, V. W. Day, R. D. Sommer, A. L. Rheingold, J. A. Belot, *Inorg. Chem.* **2001**, *40*, 5292–5295; b) D. C. Bradley, J. S. Ghoptra, F. A. Hart, *J. Chem. Soc. Dalton Trans.* **1973**, 1021–1023; c) E. C. Alyea, D. C. Bradley, R. G. Copperthwaite, *J. Chem. Soc. Dalton Trans.* **1972**, 1580–1584.
- [23] Q. Shen, W. Huang, J. Wang, X. Zhou, *Organometallics* **2008**, *27*, 301–303.
- [24] L. Zhang, S. Wang, E. Sheng, S. Zhou, *Green Chem.* **2005**, *7*, 683–686.
- [25] a) K. Komeyama, D. Sasayama, T. Kawabata, K. Takehira, K. Takaki, *Chem. Commun.* **2005**, 634–636; b) K. Komeyama, D. Sasayama, T. Kawabata, K. Takehira, K. Takaki, *J. Org. Chem.* **2005**, *70*, 10679–10687.
- [26] a) K. Komeyama, T. Kawabata, K. Takehira, K. Takaki, *J. Org. Chem.* **2005**, *70*, 7260–7266; b) M. Nishiura, Z. Hou, Y. Wakatsuki, T. Yamaki, T. Miyamoto, *J. Am. Chem. Soc.* **2003**, *125*, 1184–1185; c) M. Nishiura, Z. Hou, *J. Mol. Catal. A* **2004**, *213*, 101–106.
- [27] Q. H. Li, S. W. Wang, S. L. Zhou, G. S. Yang, X. C. Zhu, Y. Y. Liu, *J. Org. Chem.* **2007**, *72*, 6763–6767.
- [28] a) Y. Horino, T. Livinghouse, *Organometallics* **2004**, *23*, 12–14; b) T. Gountchev, T. D. Tilley, *Organometallics* **1999**, *18*, 5661–5667.
- [29] Y. Horino, T. Livinghouse, M. Stan, *Synlett* **2004**, 2639–2641.
- [30] a) Y. H. Chen, Z. Y. Zhu, J. Zhang, J. Z. Shen, X. G. Zhou, *J. Organomet. Chem.* **2005**, *690*, 3783–3789; b) M. R. Bürgstein, H. Berberich, P. W. Roesky, *Chem. Eur. J.* **2001**, *7*, 3078–3085; c) H. Berberich, P. W. Roesky, *Angew. Chem.* **1998**, *110*, 1618–1620; *Angew. Chem. Int. Ed.* **1998**, *37*, 1569–1571.
- [31] S. Seo, T. J. Marks, *Org. Lett.* **2008**, *10*, 317–319.
- [32] a) A. Motta, I. L. Fragala, T. J. Marks, *Organometallics* **2006**, *25*, 5533–5539; b) A. Motta, G. Lanza, I. L. Fragala, T. J. Marks, *Organometallics* **2004**, *23*, 4097–4104; c) J. Ryu, G. Y. Li, T. J. Marks, *J. Am. Chem. Soc.* **2003**, *125*, 12584–12605; d) Y. K. Kim, T. Livinghouse, J. E. Bercaw, *Tetrahedron Lett.* **2001**, *42*, 2933–2935.
- [33] a) A. Motta, I. L. Fragala, T. J. Marks, unpublished results; b) S. Seo, X. Yu, T. J. Marks, *J. Am. Chem. Soc.* **2009**, *131*, 263–276; c) X. Yu, S. Seo, T. J. Marks, *J. Am. Chem. Soc.* **2007**, *129*, 7244–7245.
- [34] a) S. P. Nolan, D. Stern, T. J. Marks, *J. Am. Chem. Soc.* **1989**, *111*, 7844–7853; b) D. F. McMillen, D. M. Golden, *Annu. Rev. Phys. Chem.* **1982**, *33*, 493–532; c) S. W. Benson, *Thermochemical Kinetics*, 2nd ed., Wiley, New York, **1976**, Appendix Tables A10, 11 and 22; d) M. A. Giardello, W. A. King, S. P. Nolan, M. Porchia, C. Sishta, T. J. Marks in *Energetics of Organometallic Species* (Ed.: J. A. MartinhoSimões), Kluwer, Amsterdam, **1992**, pp. 35–54; e) M. R.

- Gagné, S. P. Nolan, A. M. Seyan, D. Stern, T. J. Marks in *Metal-Metal Bonds and Clusters in Chemistry and Catalysis* (Ed.: J. P. Fackler), Plenum, New York, **1990**, pp. 113–125; f) T. J. Marks in *Bonding Energetics in Organometallic Compounds* (Ed.: T. J. Marks), ACS, Washington, **1990**, pp. 1–18; g) S. P. Nolan, D. Stern, D. Hedden, T. J. Marks in *Bonding Energetics in Organometallic Compounds* (Ed.: T. J. Marks), ACS, Washington, **1990**, pp. 159–174.
- [35] a) “The Total Synthesis of Spiroketal-Containing Products”: V. Vailancourt, N. E. Pratt, F. Perron, K. F. Albizati in *The Total Synthesis of Natural Products*, Vol. 8, 1st ed. (Ed.: J. A. Simon), Wiley-Interscience, New York, **1992**, pp. 533–691; b) F. Perron, K. F. Albizati, *Chem. Rev.* **1989**, *89*, 1617–1661.
- [36] Y. Morimoto, T. Okita, H. Kambara, *Angew. Chem.* **2009**, *121*, 2576–2579; *Angew. Chem. Int. Ed.* **2009**, *48*, 2538–2541.
- [37] A. R. Van Dyke, T. F. Jamison, *Angew. Chem.* **2009**, *121*, 4494–4496; *Angew. Chem. Int. Ed.* **2009**, *48*, 4430–4432.
- [38] A. B. Pangborn, M. A. Giardello, R. H. Grubbs, R. K. Rosen, F. J. Timmers, *Organometallics* **1996**, *15*, 1518–1520.
- [39] H. H. Fox, M. O. Wolf, R. O’Dell, B. L. Lin, R. R. Schrock, M. S. Wrighton, *J. Am. Chem. Soc.* **1994**, *116*, 2827–2843.
- [40] a) S. H. Liu, Y. Chen, K. L. Wan, T. B. Wen, Z. Zhou, M. F. Lo, I. D. Williams, G. Jia, *Organometallics* **2002**, *21*, 4984–4992; b) P. Quayle, S. Rahman, J. Herbert, *Tetrahedron Lett.* **1995**, *36*, 8087–8088.
- [41] J. L. D. De La Cruz, U. Hahn, J.-F. Nierengarten, *Tetrahedron Lett.* **2006**, *47*, 3715–3718.
- [42] J. K. Sorensen, M. Vestergaard, A. Kadziola, K. Kils, M. B. Nielsen, *Org. Lett.* **2006**, *8*, 1173–1176.
- [43] SigmaPlot 2002, version 8.0., SPSS Inc, Chicago, **2002**.
- [44] See the Supporting Information.
- [45] G. Gaefke, V. Enkelmann, S. Hoeger, *Synthesis* **2006**, 2971–2973.
- [46] a) Y. Yamanoi, H. Nishihara, *J. Org. Chem.* **2008**, *73*, 6671–6678; b) H. K. Christian-Pandya, Z. I. Niazimbetova, F. L. Beyer, M. E. Galvin, *Chem. Mater.* **2007**, *19*, 993–1001.
- [47] a) A. Wu, A. Chakraborty, D. Witt, J. Lagona, F. Damkaci, M. A. Ofori, J. K. Chiles, J. C. Fettinger, L. Isaacs, *J. Org. Chem.* **2002**, *67*, 5817–5830; b) Y. H. Lai, A. H. T. Yap, *J. Chem. Soc. Perkin Trans. 2* **1993**, 1373–1377.
- [48] G. Jeske, L. E. Schock, H. Mauermann, P. N. Swepston, H. Schumann, T. J. Marks, *J. Am. Chem. Soc.* **1985**, *107*, 8103–8110.
- [49] Representative eight-coordinate effective ionic radii: La^{III}, 1.160 Å; Nd^{III}, 1.109 Å; Sm^{III}, 1.079 Å; Y^{III}, 1.019 Å; Yb^{III}, 0.985 Å; Lu^{III}, 0.977 Å. See: R. D. Shannon, *Acta Crystallogr. Sect. A* **1976**, *32*, 751–767.
- [50] Organolanthanide-catalyzed hydrophosphinations exhibit similar but more pronounced kinetic inhibition effects, depending upon the steric bulk of the product. See: M. R. Douglass, C. L. Stern, T. J. Marks, *J. Am. Chem. Soc.* **2001**, *123*, 10221–10238.
- [51] J. I. Steinfeld, J. S. Francisco, W. L. Hase, *Chemical Kinetics and Dynamics* 2nd ed., Prentice Hall, New Jersey, **1999**; pp. 1–13.
- [52] a) P. J. Robinson, *J. Chem. Educ.* **1978**, *55*, 509–510; b) S. W. Benson, *Thermochemical Kinetics*, 2nd ed., Wiley, New York, **1986**; pp. 8–10.
- [53] Parameters in parentheses represent 3σ values derived from the least-squares fit.
- [54] For Ln³⁺-arene complexes, see: a) M. N. Bochkarev, *Chem. Rev.* **2002**, *102*, 2089–2117; b) H. Liang, Q. Shen, J. Guan, Y. Lin, *J. Organomet. Chem.* **1994**, *474*, 113–116; c) G. B. Deacon, *Aust. J. Chem.* **1990**, *43*, 1245–1257; d) B. Fan, Q. Shen, Y. Lin, *J. Organomet. Chem.* **1989**, *376*, 61–66; e) B. Fan, Q. Shen, Y. Lin, *J. Organomet. Chem.* **1989**, *377*, 51–58; f) A. Cotton, W. Schwotzer, *Organometallics* **1987**, *6*, 1275–1279; g) A. Cotton, W. Schwotzer, *J. Am. Chem. Soc.* **1986**, *108*, 4657–4658.
- [55] a) R. C. Mehrotra, A. Singh, U. M. Tripathi, *Chem. Rev.* **1991**, *91*, 1287–1303; b) H. Sheng, F. Xu, Y. Yao, Y. Zhang, Q. Shen, *Inorg. Chem.* **2007**, *46*, 7722–7724.
- [56] E. V. Anslyn, D. A. Dougherty, *Modern Physical Organic Chemistry*, University Science Books, Sausalito, **2006**, pp. 428–431.

Received: November 2, 2009

Published online: March 26, 2010